RSC Advances

REVIEW

View Article Online
View Journal | View Issue

Cite this: *RSC Adv.*, 2023, **13**, 28307

Recent progress, trends, and new challenges in the electrochemical production of green hydrogen coupled to selective electrooxidation of 5-hydroxymethylfurfural (HMF)

Leyla Gidi,[a] John Amalraj,[*a] Claudio Tenreiro[b] and Galo Ramírez[cd]

The production of clean electrical energy and the correct use of waste materials are two topics that currently concern humanity. In order to face both problems, extensive work has been done on the electrolytic production of green H_2 coupled with the electrooxidative upgrading of biomass platform molecules. 5-Hydroxymethylfurfural (HMF) is obtained from forest waste biomass and can be selectively oxidized to 2,5-furandicarboxylic acid (FDCA) by electrochemical pathways. FDCA is an attractive precursor to polyethylene furanoate (PEF), with the potential to replace petroleum-based polyethylene terephthalate (PET). An integrated electrochemical system can simultaneously produce H_2 and FDCA at a lower energy cost than that required for electrolytic water splitting. Here, the benefits of the electrochemical production of H_2 and FDCA over other production methods are presented, as well as the innovative applications of each reaction product and the advantages of carrying out both reactions in a coupled system. The recently reported progress is disclosed, through an exploration of electrocatalyst materials used in simultaneous production, including the use of nickel foams (NF) as modification substrates, noble and non-noble metals, metal non-oxides, metal oxides, spinel oxides and the introduction of oxygen vacancies. Based on the latest trends, the next challenges associated with its large-scale production are proposed for its implementation in the industrial world. This work can offer a guideline for the detailed understanding of the electrooxidation of HMF towards FDCA with the production of H_2, as well as the design of advanced electrocatalysts for the sustainable use of renewable resources.

Received 17th August 2023
Accepted 15th September 2023

DOI: 10.1039/d3ra05623f

rsc.li/rsc-advances

1. Energy and climate contextualization

1.1 Problems associated with the use of fossil fuels and forestry activities

The production of electric power has become essential to meet the growing energy demand of today's societies. This brings challenges associated with the problem of climate change along with the depletion of non-renewable energy sources such as coal, gas, and oil.[1,2] It is estimated that if these natural resources continue to be consumed at the current rate, in the near future it will no longer be feasible to supply the growing global energy requirement.[3] Indeed, at current levels, fossil energy consumption appears strongly unsustainable. Besides the Intergovernmental Panel on Climate Change (IPCC) highlights with a high level of confidence that global warming is likely to reach +1.5 °C between 2030 and 2052 if it continues to increase at current rates.[4] An energy transition is being implemented in most regions, charting an energy transition path that could lead from the current fossil fuel-based system to an affordable, efficient, sustainable, and environmentally safe energy future.[5]

Added to this energy and ecological situation is the problem of the accumulation of waste resulting from permanent industrial activity. Specifically, the forestry industry generates large amounts of biomass waste, increasing the risk of environmental crisis.[6] These biomass residues derived from forestry operations and wood manufacturing can be used to produce biofuels and biomaterials as sustainable alternatives to drive the development of renewable technologies and the bio-economy.[7]

As a way of anticipating future energy, economic, and environmental needs, work has been done on estimating the world renewable energy market. In this sense, according to Renewable Energy Market – Analysis, Size & Report – Industry Overview.[8] The size of the renewable energy market is expected to grow from 3.96

[a]*Laboratory of Material Science, Chemistry Institute of Natural Resources, Universidad de Talca, P.O. Box 747, Talca 3460000, Chile. E-mail: jamalraj@utalca.cl*
[b]*Industrial Technologies Department, Faculty of Engineering, Universidad de Talca, Curicó 3340000, Chile*
[c]*Departamento de Química Inorgánica, Facultad de Química y de Farmacia, Pontificia Universidad Católica de Chile, Av. Vicuña Mackenna 4860, Santiago 7820436, Chile*
[d]*Millenium Institute on Green Ammonia as Energy Vector (MIGA), Av. Vicuña Mackenna 4860, Macul, Santiago 7820436, Chile*

terawatts in 2023 to 5.58 terawatts in 2028, at a Compound Annual Growth Rate (CAGR) of 7.09% during the period studied (2023–2028). This market report addresses global renewable energy, market, growth, size, and trends, and is segmented by type including solar, wind, hydro, bioenergy, and others (geothermal, tidal, *etc.*). The report also involves geography covering North America, Asia-Pacific, Europe, South America, and Middle-East and Africa. Additionally, the report of Renewable Energy Market Size, Share Analysis | Grow Forecast – 2030,[9] indicates that the global renewable energy market was valued at $881.7 billion in 2020, and is projected to reach $1977.6 billion by 2030, growing at a CAGR of 8.4% from 2021 to 2030. This analysis covers hydroelectric, wind, bioenergy, solar, and geothermal types of energy including the regions of North America, Europe, Asia-Pacific, and LAMEA.

During the last decades, great efforts have been made on the generation of clean energy through renewable resources.[10–13] As an example, solar and wind renewable sources have been widely studied, but unfortunately, both depend on climatic circumstances and the availability of large-scale energy storage systems.[14,15] In this sense, it is urgent to study and develop other kinds of energy production systems, such as those related to electrochemistry, which provide a promising alternative to generate and storing energy in large proportions.[16–18] In this way, it is attractive to work on the search for sustainable solutions through coupled electrochemical systems that allow the production of clean energy and at the same time convert biomass waste to use.

1.2 H_2 as an energy alternative

Molecular hydrogen (H_2) is a promising fuel that can be used in various energy storage and conversion systems.[19,20] Within the alternatives presented by electrochemistry, the production of green H_2 is acquiring great prominence. H_2 gas has a very high energy density whose value is close to 142 MJ kg^{-1} and also has a high calorific value which is three times heat release per unit mass more than gasoline.[21] After the combustion of H_2, the only by-product generated is water, which makes it highly clean. As in combustion does not produce greenhouse gases, it offers great potential to reduce CO_2 emissions into the atmosphere. Hydrogen is considered the most abundant element in the universe, despite this, it is very difficult to find it by itself in its gaseous form as H_2, and in order to obtain it, it must be produced artificially.[22]

H_2 can be classified according to its production method through colors (grey, blue, turquoise, and green), which also indicates how clean these methods are. In this way, the impact of H_2 production on the environment can be identified.[23]

In general, production processes that generate the greatest amount of carbon are classified as grey. "Grey H_2" can be produced by coal gasification, steam reforming of methane, partial oxidation of methane gas, or through methane decomposition. Although these techniques are cheaper, they emit high amounts of carbon into the ecosystem, so they do not meet the expectations of producing clean energy.[24] When the methods involve techniques to capture and store carbon, they are classified as blue. In the case of "blue H_2", the same production methods are used as grey H_2 but carbon capture and storage processes are incorporated, making H_2 production a little cleaner.[25] When H_2 is obtained by pyrolysis of methane, it is called "turquoise H_2". In this case, despite the fact that the primary feedstock is still natural gas, the process is free of CO_2 emissions.[23] On the other hand, methods that do not require natural gas as a starting material and also do not generate carbon emissions are considered cleaner. For example, "red H_2" is the one that originates in nuclear power plants through electrolysis of water using nuclear energy. Although these methods do not produce CO_2 emissions into the environment, they do generate nuclear waste and therefore cannot be considered 100% clean.[26] Finally, "green H_2" is the cleanest, as it involves the production of H_2 solely from methods that use electricity to split H_2O molecules into H_2 and O_2, such as electro- and photoelectrocatalysis or similar methods. Additionally, the fundamental requirement for H_2 to be considered "green" is that it be produced using electricity obtained from renewable sources, among which solar, wind and hydraulic sources stand out.[27–30] Green H_2 production promises to be the "clean energy of the future", yet large-scale production remains expensive.[31] Table 1 presents a summary for the classification of H_2 by colors according to the resources used for its production, the process of obtaining it and CO_2 emissions into the atmosphere.

The global industry, size, share, growth, trends and forecast analysis of hydrogen-based renewable energy market has also been detailed through the Hydrogen-based Renewable Energy Market.[32] The technologies considered are Alkaline Electrolyte Cell (AEC), Polymer Electrolyte Membrane (PEM) and Anion Exchange Membrane (AEM) for its application in transport, chemical and petrochemical, petroleum refinery, steel, mining, power generation, heat generation and others. Through the report submitted in the study period 2022–2031, the global hydrogen-based industry was valued at $776.3 million in 2022 and it is estimated to advance at a CAGR of 49.7% from 2023 to 2031, reaching $5.3 billion by the end of 2031. Moreover, according to Green Hydrogen Market Analysis & Future Trends Report,[33] the world market for green hydrogen was valued at $676 million in 2022 and is projected to reach $7314 million by 2027, growing at a CAGR 61.0% from 2022 to 2027. This Green Hydrogen Market report is based on hydrogen obtained from alkaline electrolysis and PEM electrolysis technologies using renewable resources such as wind energy, solar energy and others (geothermal, hydropower and hybrid of wind and solar).

1.3 Current and potential applications of H_2

Currently it is possible to obtain electrical energy from H_2 in fuel cells, which are electrochemical devices that work in a similar way to batteries, producing electrical energy from electrochemical reactions. Fuel cells have a cathode where a reduction reaction of an oxidizing species occurs and an anode where the oxidation of a fuel occurs. Both electrodes (cathode and anode) are connected through an external circuit. Within the different types of fuel cells, the proton exchange membrane (PEM) technology has been one of the most developed.[34,35] According to Fig. 1, the Hydrogen

Table 1 Color code used for H_2 (grey, blue, turquoise, red and green) according to its source, production process and resulting CO_2 emissions

Color	"Grey"	"Blue"	"Turquoise"	"Red"	"Green"
Source	Methane or coal	Methane or coal	Methane	Water and nuclear energy	Water and renewable energy
Process	SMR[a] or gasification	SMR[a] or gasification with carbon capture	Pyrolysis	Electrolysis	Electrolysis
Resulting CO_2 emissions	High CO_2	Low CO_2	Relatively CO_2 free	Carbon-free	Carbon-free

[a] SMR: steam methane reforming.

Oxidation Reaction (HOR) occurs at the anode where the reduction of H_2 to protons (H^+) occurs which react with gaseous oxygen O_2 to form water as a clean product of the reaction in the cathode through the Oxygen Reduction Reaction (ORR). H_2 in this case acts as fuel.[36]

In fact, there are already vehicle engines that work through the combustion of H_2 to replace gasoline from petroleum. Automakers like Honda, Toyota, and Hyundai have started manufacturing fuel cell vehicles using H_2 as fuel.[37] These vehicles are already available in North America, Asia and Europe.[38]

As of June 2018, more than 6500 fuel cell vehicles had been sold. At that date, California showed its leadership in the sale of this type of vehicle, with almost 3000 units, due to the fact that the state houses the largest network of H_2 service stations in the world.[37] Several automakers are promoting their fuel cell vehicles to customers, who often buy battery electric vehicles. Both types of vehicles are characterized by producing zero greenhouse gas emissions and are capable of being powered by renewable, sustainable and, above all, clean energy sources.[37] H_2 has increasing potential for use as a fuel in the future. In fact, it is estimated that by the year 2030 the cost of fuel cells will be comparable to traditional gasoline-powered vehicles, due to the impressive technological advances of recent years and the advantages that are observed today with respect to availability.[39]

The application of fuel cells has been proven for all types of transport. For example in shipping, fuel cells have been used for many years in major propulsion power and auxiliary power unit applications.[40] Using H_2 as fuel, the PEM fuel cell has been popular in marine vehicle projects due to its high energy efficiency and anti-pollution impact.[41]

Air transport shows a participation in world energy consumption between 2.5% and 5% in total and showing a growing perspective of approximately 4.8% per year.[42] The first work on the use of H_2 fuel in aircraft was took place in 1956 when the United States began flying a bombed-out B57

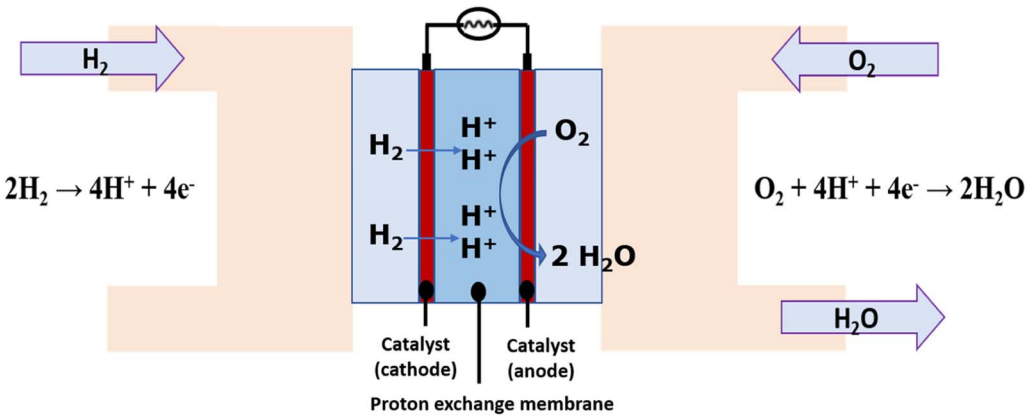

Fig. 1 Operation of a PEM fuel cell.

Canberra aircraft that used helium-pressurized H_2 fuel in one of its engines.[43] The work of NASA has allowed the merger of the aviation industry and H_2 energy, placing fuel cells in a prominent position for their development in aircraft.[42] Both fuel cells and batteries are environmentally friendly devices that can be used in air transportation.

However, on the one hand, the battery contains a closed energy store inside it and forced to the charge/discharge situation with an external supply of electricity for the electrochemical reaction to occur on the contrary. A fuel cell, on the other hand, uses an external supply of chemical energy and can operate indefinitely using H_2 and O_2 sources.[44] The key to aircraft being able to run on H_2 is to continue to move towards storage issues as it takes a lot of liquid H_2 for an aircraft to fly.[42,45] Additionally, during the H_2 generation, the use of fossil fuels continues to limit the effectiveness of production. It is predicted that the easiest and most cost-effective way to use H_2 for aircraft fuel is from nuclear power.[42]

H_2 has also had its applications in aeronautics at the beginning of the 20th century, for rigid aircraft such as Zeppelin due to its excellent rebound characteristic.[46,47] Subsequently, the development of aircraft using H_2 as propellant has been evaluated in many countries, such as Suntan (USA-1956), Tupolev Tu-155 (Soviet Union-1988), CRYOPLANE (Europe-2000), HyShot (Australia-2001), NASA X-43 (USA-2004), Phantom Eye (USA-2013). Also, H_2 is the main rocket fuel due to its high specific energy. A rocket fuel tank is normally filled with liquid H_2 and liquid O_2 which react together and give a lot of power to propel the rocket.[47] H_2 fuel technology is so promising that work is under way to develop high-performance fuel cells in the aerospace sector. Specifically regenerative fuel cells can collect and store solar energy during the day and gradually release it when needed, making power available 24/7.[48]

Although there is abundant information about the current and possible applications of H_2 technology in transportation (land, sea, air and space), the literature hardly addresses its implementation in the industrial sector. H_2 could potentially be applicable in sustainable factory systems. Given that the industrial sector is the second largest emitter of greenhouse gases in the world, there is an urgent need to find new alternatives to decarbonize factory systems. H_2 could be widely applicable in factories both in electricity and heat generation as process gas or fuel. This is a potential pathway to move factories towards carbon neutrality.[49] As an example, in 2018, the steel-making factory consumed 3.75 GW h of energy from coal, which corresponds to 32.5% of the total coal consumption.[50] Therefore, the use of renewable energy in this industry will significantly reduce greenhouse gas emissions. For factories to make the decision to change energy sources, certain critical parameters must be analyzed: the calorific value of coal (22 MJ kg^{-1}) is relatively low compared to the calorific value of H_2 (142 MJ kg^{-1}). Therefore, H_2 handling processes will be easier than coal. Safety, toxicity and environmental effects are usually minor concerns for a factory as high level precautions are taken. Due to the fact that the energy supply must be continuous, the economic cost factor is one of the most relevant parameters in decision making. This indicates that the decrease in H_2 production costs is the main challenge for its application at an industrial level.[50]

In order to make the production and application of H_2 economically more attractive for the various factories, there is the possibility of coupling the electrochemical production of H_2 to the simultaneous generation of high-value molecules for the industrial sectors. The benefits of this promising alternative are explained in detail below.

2. H_2 production coupled to oxidation of industrial interest molecules

According to the above green H_2 classification, gaseous H_2 can be produced by the electrochemical breakdown of water molecules through a process called electrolysis (Fig. 2a). For the splitting of the water molecule to occur, the application of a continuous electric current is required through two electrodes, the cathode, and the anode. At the cathode, the hydrogen evolution reaction (HER) occurs, which consists of the reduction of H^+ to H_2, while at the anode, the oxygen evolution reaction (OER) occurs, corresponding to the oxidation of H_2O to O_2. Both reactions occur simultaneously, and the electrons are transferred from the anode to the cathode through an external circuit.[51] The H_2 production (HER) has many advantages, however, the O_2 production (OER) is an unattractive reaction, since it generates a product of little value (O_2). On the other hand, the rate of the process is limited by the rate of the oxidation reaction (OER), which has slow kinetics, for the production of green H_2. This means that a greater magnitude of overpotential is required for the OER than that used in the HER, thus reducing the energy conversion efficiency of the entire process.[52] One way to avoid this limitation is to replace the production of O_2 with an energetically more favorable oxidation reaction, which supplies electrons for the HER to occur simultaneously and which also allows the generation of an oxidation product with higher added value at the anode.[52]

As shown in Fig. 2b, it is possible to use a two-compartment cell separated by a membrane, where the oxidation of an alternative molecule is generated on the anode as a replacement for the production of O_2. In the search for molecules that are oxidizable at a lower overpotential and that also present benefits over the production of O_2, the idea of taking advantage of certain platform molecules obtained from biomass to generate chemical products with higher added value is proposed.

Biomass waste valorization processes integrate conversion procedures of its components, to obtain higher value products, such as fuels and some chemical products, and it is crucial to guarantee a carbon-based circular economy in the future, with economic and environmental benefits. In this context, lignocellulosic biomass, known to be the raw material for the pulp and paper industry,[53] is very abundant and has the capacity to produce liquid fuels and numerous compounds of industrial interest.

There are several platform molecules from forest biomass that are interesting to couple their oxidation to the electrolytic

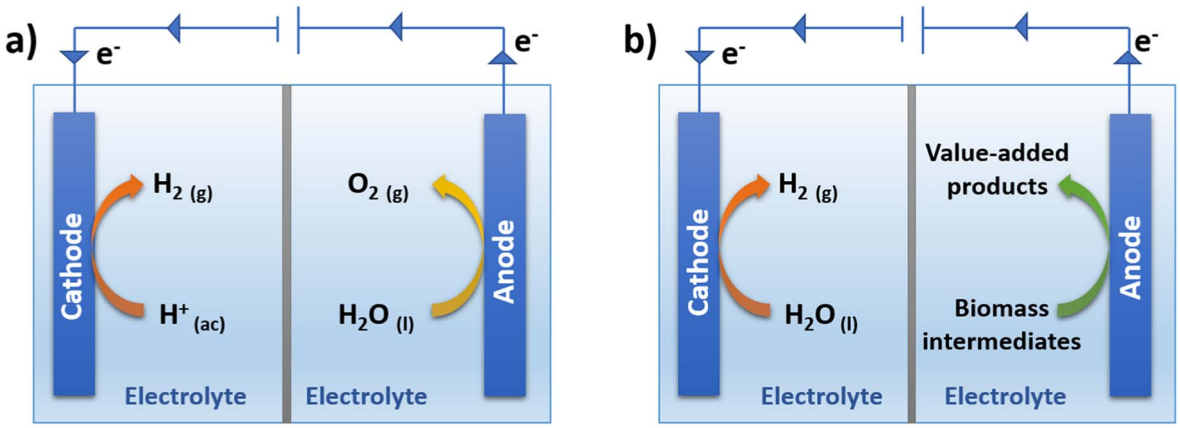

Fig. 2 (a) Traditional water electrolysis with simultaneous O_2 and H_2 production, (b) simultaneous production of H_2 and value-added products.

production of H_2. Among the different platform molecules obtained from forest biomass that can be valorized by electrochemical routes through oxidation, the 5 most prominent are ethanol, benzyl alcohol, furfural, furfuryl alcohol and 5-hydroxymethylfurfural (HMF),[54] which correspond to representative organic substrates for their simultaneous electrocatalytic oxidation to the production of H_2 from electrochemical splitting of water.

Below are the typical technical problems[54] associated with traditional water electrolysis:

(1) Conventional water electrolyzers produce H_2 and O_2 gases simultaneously, so it is necessary to include additional methods of separating these gases and thus avoid the formation of the mixture of H_2/O_2, which can be explosive.

(2) The possible formation of reactive oxygen species (ROS) can cause the degradation of cell membranes, prematurely damaging electrochemical devices, decreasing their useful life considerably.

On the other hand, the integration of the electrochemical oxidation of these 5 biomass intermediates in replacement of the OER entails multiple benefits,[54] among which the following stand out:

(1) The electrical energy consumption required for the production of H_2 can be significantly reduced due to the use of more thermodynamically convenient organic reagent oxidation reactions, thus increasing the energy conversion efficiency.

(2) The production of value-added fine chemicals from electrochemical reactions maximizes investment in economic and energy terms.

(3) Because the anode products are generally non-gaseous, membrane less electrolysis can be achieved.

(4) Electrochemical oxidation of biomass intermediates produces valuable products with higher energy conversion efficiency than traditional water splitting.

It should be noted that biomass is the only green and truly sustainable carbon source. The conversion of biomass into fuels and chemicals, often called "biorefinery", is seen as a promising and increasingly viable alternative to replace current oil refining processes.

One of the 5 platform molecules obtained from biomass that draws particular attention is 5-hydroxymethylfurfural (HMF). HMF is the dehydration product of C_6 carbohydrates and can act as a precursor for the synthesis of a wide variety of valuable chemicals, plastics, pharmaceuticals, and even liquid fuels and its commercial price is 20–50 $ per kg. One of the HMF oxidation products that generates the most interest due to its high added value is 2,5-furanedicarboxylic acid (FDCA).[54]

FDCA is a monomer that has received increasing attention in the industry, and is being referred to as a "green" chemical platform that can be transformed into a number of high-value biobased chemicals such as polyesters, polyamides, plasticizers, and drugs[55–57] through various synthesis methods.[58–60] FDCA is priced at 10–25 $ per kg and is on the US Department of Energy (DOE) list of top 15 molecules that have the potential to replace monomers obtained from the petroleum industry such as terephthalic acid (TPA),[61–63] due to their great structural similarity. The polycondensation reaction of FDCA with ethylene glycol produces poly(ethylene furanoate) (PEF), with a yield greater than 90%.[64] PEF has superior mechanical properties, better gas barrier properties, and lower non-renewable energy consumption compared to PET.[65–67]

Additionally, FDCA has been copolymerized with aliphatic and cyclic acid comonomers to improve biodegradability. These copolyesters have demonstrated excellent gas barrier and thermomechanical properties, making them suitable candidates for food and beverage packaging.[62] For this reason, it is crucial to propose selective production of FDCA by electrochemical pathways, for the industrial production of PEF. This will make it possible to reduce the current generation of plastic products from petroleum.

Through the electrochemical oxidation methodology of HFM to obtain FDCA, plastic products such as food and beverage packaging can be obtained from biomass residues, using materials that have been considered as forestry industry waste, favoring the circular economy and drastically reducing the carbon footprint. Fig. 3 shows a summary of the steps to obtain food and beverage packaging from biomass waste, including (a) dehydration of C6 carbohydrates obtained from biomass, (b)

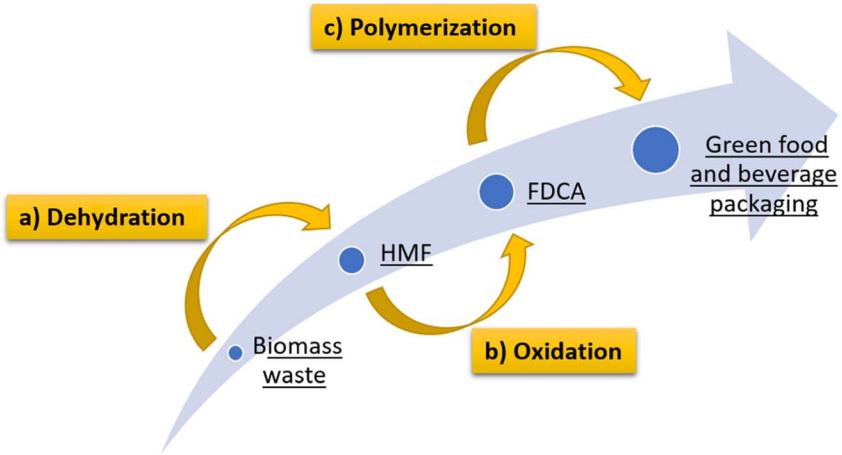

Fig. 3 Steps involved in obtaining food and beverage packaging. (a) dehydration of C6 carbohydrates obtained from biomass, (b) oxidation of HMF to FDCA and (c) polymerization treatments.

oxidation of HMF to FDCA and (c) polycondensation and copolymerization treatments for the manufacture of containers for food and beverages.

The catalytic oxidation of HMF is the main route of production of FDCA. The main approaches to catalysis are thermal catalysis, biocatalysis, electrochemical catalysis, and photocatalysis. Among these production methods, thermal catalysis has been reported most frequently. The catalytic oxidation of HMF with noble metals can obtain an excellent conversion rate, but the high cost of the materials does not favor its application at the industrial level.[68]

There are several industries involved in the production of FDCA.[62] For example, Avantium and BASF, under a joint venture (Synvina), successfully studied and improved the separation and selectivity of catalysts in the production of FDCA. At the beginning of 2020, Avantium signed a memorandum of understanding to locate a pilot plant in the Netherlands with a goal of obtaining 5 kilotons of product through a technology that consists of the dehydration of carbohydrates in an alcoholic medium to form alkoxymethylfurfural or methoxymethylfurfural and methyllevulinate, and its subsequent oxidation to FDCA using acetic acid. These steps are followed by the polymerization of FDCA with ethylene glycol to form PEF.[69] Additionally, Dupont, Archer Daniels Midland Company, Origin Materials and Eastman Company, AVA Biochem and the VTT Research Center have also innovated in the development of new technologies for the production of FDCA at a commercial level.[62] The Petrobras company implemented a process for the conversion of sugars into HMF using an ion exchange resin, followed by oxidation to FDCA.[70] Despite these advances, there are still challenges that prevent the large-scale production of FDCA, since it is possible to produce a low amount of FDCA and the reaction times are very long.[71] Most of these companies opt for FDCA production processes focused on the use of heterogeneous catalysts and green solvents.[37]

Although great efforts have been made to reduce the impact on the environment, the classic methodology used in the industry for the oxidative transformation of HMF to FDCA is still carried out with large amounts of strong chemical oxidants. Furthermore, expensive catalysts and production methods are used to obtain its numerous oxidation products.[72–74] These methods also involve hard reaction conditions, including for example the use of high pressure O_2 (greater than 10 bar) and temperatures above 80 °C.[74] Building a cheap and efficient catalytic system to oxidize HMF under mild conditions remains a challenge pursued by industry and researchers. Considering the above, electrocatalytic oxidation is a more sustainable alternative since the conversion occurs by the application of electricity and costly or environmentally harmful chemical oxidants are not needed. Electrocatalysis is a cleaner, safer and more controllable form of catalysis where reaction parameters such as current potential and voltage can be adjusted more conveniently and precisely.[68]

2.1 Electrolytic H_2 production coupled to electrovalorization of 5-hydroxymethylfurfural (HMF)

HMF is a furan ring system with formyl and hydroxymethyl groups and can be converted to high-value chemicals. Conventional thermocatalytic oxidation of HMF to high value chemicals such as HMFCA (5-hydroxymethyl-2 furan carboxylic acid), FFCA (5-formyl-furoic acid), DFF (diformyl furan) and FDCA (2,5 furan dicarboxylic acid) is generally carried out over supported Pt, Au, Pd and Ru catalysts at high temperature and in high pressure oxygen atmosphere.[75] Although cheaper transition metal-based catalysts have been designed and used, their catalytic activity is typically lower than that of noble metal-based catalysts.[75–80]

An electrocatalytic reaction is a chemical reaction system driven by an electrochemical potential. Specifically, it refers to the process of gaining electrons at the cathode for the reduction reaction and losing electrons at the anode for oxidation under the action of voltage.[81–83] The electrocatalytic reaction is activated when the applied external voltage reaches the overpotential required for the reaction to occur.[82]

Fig. 4 shows a scheme for the electrochemical oxidation of HMF to FDCA in three steps, through two possible reaction

pathways (DFF or HMFCA, which are further oxidized to FFCA and finally to FDCA).[84] The entire process, independent of the oxidation pathway, involves a transfer of 6 electrons in total. The two possible steps presented in Fig. 4 involve the following events:

(i) The hydroxymethyl group of HMF is oxidized to DFF, which is further oxidized to FFCA and finally to FDCA (HMF → DFF → FFCA → FDCA).

(ii) The formyl group of HMF is initially oxidized to HMFCA and then the hydroxymethyl group of HMFCA is oxidized to FFCA. Finally, the formyl of FFCA is oxidized to form FDCA (HMF → HMFCA → FFCA → FDCA).

In addition to electrocatalytic reactions, there are photoelectrocatalytic reactions, which usually use electrodes made of semiconductor materials in order to produce charge carriers (*i.e.*, pairs of holes and electrons) by irradiating light. Holes in the valence band (VB) as oxidizing species can facilitate the electrochemical oxidation of compounds, and electrons in the conduction band (CB) as reducing species can facilitate the electrochemical reduction of compounds.[70] Both electrocatalytic and photoelectrocatalytic reactions are generally carried out under soft conditions and have the advantages of ecology, sustainability, and energy saving.[85,86]

A wide variety of highly efficient electro- and photoelectrocatalysts have recently been developed and synthesized to perform the electrochemical oxidation of HMF to high-value products at medium and low voltages.[86] Both electrocatalytic and photoelectrocatalytic oxidation of HMF in high-value chemicals have attracted wide attention.[71,74,87,88]

One of the main advantages of carrying out the oxidation of HMF by electrochemical means is the high selectivity towards obtaining FDCA as the only reaction product.[89] As shown in Fig. 5 it is possible to simultaneously perform the electrochemical oxidation of HMF to form FDCA and the hydrogen evolution reaction (HER), while increasing the energy efficiency of H_2 production,[54] given the ability of HMF to oxidize at a lower overpotential than that required by the OER.[90]

As shown in Fig. 5, the reaction to produce FDCA at the anode is given by eqn (1).

$$HMF + 6OH^- \rightarrow FDCA + 4H_2O + 6e^- \quad (1)$$

Similarly, the cathodic reaction in eqn (2) involves the electrolytic production of H_2.

$$6H_2O + 6e^- \rightarrow 3H_2 + 6OH^- \quad (2)$$

Finally, the global reaction for the simultaneous production of H_2 and FDCA is expressed by eqn (3).

$$HMF + 2H_2O \rightarrow FDCA + 3H_2 \quad (3)$$

Both of these coupled reactions are generally carried out in 3-compartment electrochemical cells suitable for using a counter electrode, a reference electrode, and a working electrode upon which formation of the desired products occurs. Through a study of linear or cyclic voltammetry, it is possible to visualize the starting potential, whose value indicates how good an electrocatalyst the working electrode is. The lower the energy requirement in terms of electrochemical potential for the conversion to begin, the higher the electrocatalytic activity of the working electrode.

Both coupled reactions are most often carried out in an alkaline 1 M KOH solution as the electrolyte, since under acidic conditions (pH < 2–3) FDCA is not soluble in aqueous media and precipitate formation begins to occur. Despite this, there are works in which the electrooxidation of HMF to FDCA in an acid medium has been proposed as an alternative way to more easily isolate FDCA from solutions by a simple filtration process.[91] In any case, it is important to consider that the electro-oxidation of any organic molecule involves a series of stages associated with electrons coupled to protons and therefore the pH value has a great relevance in the reactivity, which is expected to be maximum at a pH close to the pK_a of compound.[92–97] Given the pK_a of HMF of 12.8, it is key to work under alkaline conditions to ensure the maximization of the electrocatalytic activity of HMF against nucleophilic attack by OH^-. Therefore, to ensure high yield and selectivity, pH optimization should be performed.[98]

The electrovalorization of HMF has been carried out experimentally, achieving a selectivity towards the production of FDCA of 100% (ref. 99 and 100) or values very close to 100%.[101–106] When the conversion of HMF does not proceed completely to the formation of FDCA, other intermediates such as DEF, HMFCA,

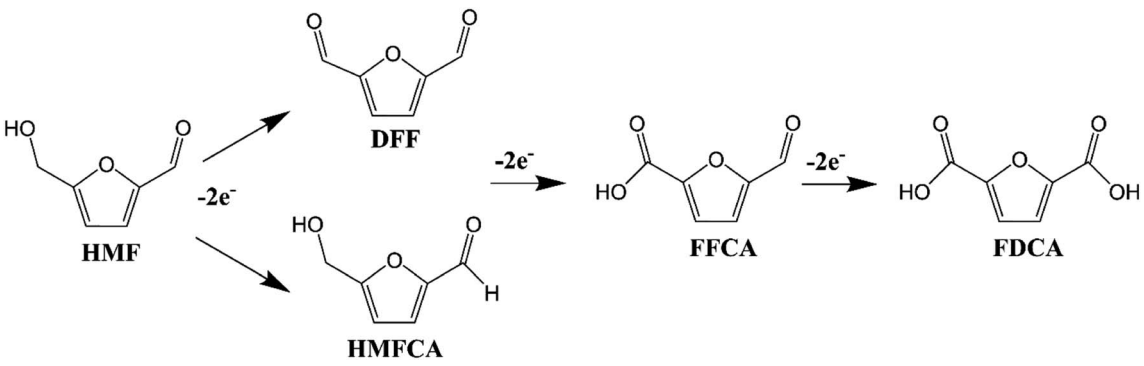

Fig. 4 Oxidation scheme of HMF to FDCA (2,5 furan dicarboxylic acid) in 3 steps, with an exchange of 6 total electrons, through two possible routes: *via* DFF (diformyl furan) and *via* HMFCA (5-hydroxymethyl-2 furan carboxylic acid), where FFCA (5-formyl-furoic acid) is intermediary.

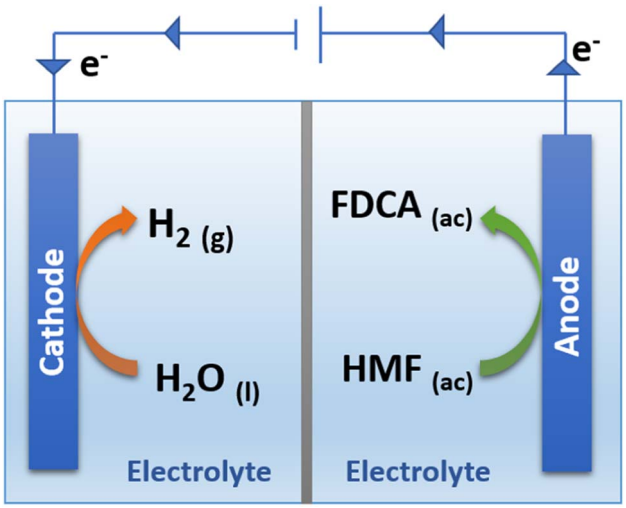

Fig. 5 Simultaneous production of H_2 and 2,5-furandicarboxylic acid (FDCA).

and FFCA are often formed[107] (see Fig. 4) which can be quantified by High Performance Liquid Chromatography (HPLC) (see Section 4: Conversion and distribution in the production of H_2 and FDCA).

3. Electrolytic H_2 production assisted by biomass and other H_2 production methods: feasibility and viability

Considering non-renewable hydrogen production routes, Steam Methane Reforming (SMR) is a classically used process providing more than 80% of the hydrogen generated worldwide.[108] Despite the fact that this technology presents a high energy efficiency (74–85%), the use of fossil fuels continues to be a great disadvantage. In this sense, it is required to use additional equipment and energy to capture a percentage of the CO_2 released,[109] therefore this and other technologies based on fossil fuels are neither green nor sustainable.[110] Pyrolysis is another classical route of hydrogen production, but it still presents low yields, separation and purification problems, tar deposition, and high hydrogen production costs.[111] Like SMR, pyrolysis requires the installation of auxiliary equipment to treat contaminants.[110,112]

Regarding renewable routes, the biohydrogen process is considered non-polluting and can be easily carried out at atmospheric pressure and temperature with a high energy content (120 kJ g^{-1}).[113] However, biohydrogen production faces low hydrogen yield,[114] high moisture content, separation and purity problems, and energy feed problems.[115,116] Therefore, more research is needed to commercially introduce the biohydrogen process.[110]

Photocatalysis is a clean and environmentally safe H_2 production technique, but it still faces a major challenge associated with the preparation of a suitable semiconductor material as a catalyst, which is abundant, cheap and easy to regenerate.[117] Water electrolysis from renewable and sustainable sources, is considered a reasonably efficient method as it provides 4% of the total hydrogen production worldwide.[118] The most significant advantage of this technology is that it does not require H_2 separation. However, the main challenge of electrolysis is the cost-effective production of hydrogen given its high energy consumption.[110] For this reason, water electrolysis has not yet been able to manifest itself economically above SMR. Water electrolysis produces hydrogen with an energy efficiency of up to 52% with the corresponding cost of 10.3 $ per kg.[119] Water electrolysis produces 380 000 kg of H_2 per year and the consumption is 53.4 kW h per kg of H_2.[120] The production rate has been determined to be 20 g kW^{-1} h^{-1} with an expected cost and efficiency of 0.09 € per kW per h or 6.36 $ per kg and 79.2%, respectively.[121] Alkaline water electrolysis is currently the cheapest way to produce electrolytic grade hydrogen (~700–800 € per kW).[122] It is estimated that water electrolysis could become profitable soon if the costs of renewable energy decrease because it does not require any other raw materials besides water.[110]

An important point to consider is that unlike water electrolysis assisted by electrooxidation of organic molecules, traditional water electrolysis uses expensive devices to avoid the crossover of H_2 and O_2 gases, making the production cost of H_2 two or three times greater than that of reforming fossil fuels.[123,124] Also, from the hydrogen production cost perspective, water electrolysis generally requires an electricity input of at least 4 kW h N m^{-3} H_2,[125,126] while water electrolysis assisted by electro-oxidation of organic molecules could reduce consumption of electricity below 4 kW h N m^{-3} H_2.[127] Therefore, the electrolytic production of hydrogen assisted by electro-oxidation of organic molecules such as biomass does not require the use of expensive separators of H_2 and O_2, reduces energy consumption and also produces molecules of industrial interest at the anode with clear commercial benefits, demonstrating its economic superiority and feasibility over traditional water electrolysis.

4. Exploration of materials used in the simultaneous electrochemical production of H_2 and FDCA

For several decades it has been possible to carry out the traditional electrolysis of water to produce H_2 efficiently on platinum electrodes with overpotentials close to zero.[128] However, to meet the growing energy demand, cheaper electrocatalysts are required, and they are more widely available and abundant on earth. An intense and growing search for materials that can replace platinum has been carried out and, in this exploration interesting alternatives have been found related to the use of nanoparticles doped with heteroatoms on noble metals.[129,130] Likewise, palladium electrodes supported on nitrogen-doped CNTs (Pd/N–CNT),[131] or systems of phosphorus-doped graphene (Pd/PG) and phosphorus-doped carbon nanoparticles (Pd/P–CNP)[132,133] have shown an electrocatalytic activity comparable to that of platinum for HER, however, the use of noble metals remains highly expensive.[134]

In order to reduce the cost of electrocatalysts for traditional H_2 production from water, carbon supports such as glassy carbon or materials related to graphite[51] have been used, as well as complexes that present transition metals, such as metallic tetraphenylporphyrins,[135] or as in the case of some Cu[136] and Co[137] porphyrins.

It has seen previously that the energy cost of H_2 production can be reduced by replacing the anodic reaction of oxygen production with the oxidation of other molecules such as HMF present in the biomass. The search for bifunctional materials to simultaneously electrocatalyze the production of H_2 and FDCA has been a constant challenge for science and industry.

Electrochemical oxidation of HMF to FDCA using nickel oxide/hydroxide electrodes was first reported by G. Grabowski *et al.* (1991) using a two-compartment electrochemical cell.[138] A strongly alkaline electrolyte (1 M NaOH) was used at a current density of 16 mA cm^{-2}. In this work, a yield of 71% of FDCA was obtained. However, the electrochemical oxidation of HMF was not studied again until several years later, probably because the importance of FDCA was not well recognized by the academic community.[139] Electrocatalysts of noble metals and their alloys were subsequently published. Subsequently, there has been a growing wave of research related to materials science, in a constant search to reduce the energy and economic cost of the electrodes in the electrocatalytic oxidation of HMF. Advances in electrocatalysis have made it possible to manufacture bifunctional materials that can carry out HMF and HER oxidation simultaneously, however, the stability and performance of HER has yet to be improved.[54,140]

Below are some materials that have been widely used as electrodes in the electrocatalytic oxidation of HMF to produce FDCA. It is highlighted the use of nickel foam (NF) as modification substrate, noble metals, non-noble metals, metal non-oxides, metal oxides, spinel oxides and the introduction of oxygen vacancies. Many of these materials function as bifunctional electrocatalysts in the simultaneous production of H_2 and FDCA, however, only the information associated with the production of FDCA is shown, since as mentioned above, the electrical energy in terms of onset potential required for the production of H_2 can be significantly reduced due to the organic reagent oxidation reactions as HMF replacing the O_2 evolution, since being thermodynamically more convenient, it is capable of increasing the efficiency of the energy conversion of H_2 production.

4.1 Use of nickel foam as a modification substrate

Nickel foam (NF) is a 3D porous metal substrate whose specific surface area is quite high due to its varied hierarchical pore structures.[141] Nickel foams are used as an electrode material because they offer excellent cycle stability, are inexpensive, highly conductive of electrical current, and have outstanding surface area. NFs are considered good electrode materials because they enhance the available active surface area on the substrate and improve the interactions between electrolyte ion diffusion and the substrate and are chemically stable in numerous liquid electrolytes.[142,143] Its abundant number of tiny holes and criss-cross channels within the foam act as a pathway for the transport of ions and electrons. In this context, they provide effective networks for efficient electron collections and excellent channels for electrolyte/ion diffusion. These holes and channels also allow to improve the surface area of the electrodes.[144–146] At the same time, porosity ensures economical use of the material and improves the accessibility of the reagents. Therefore, they are widely used as active substrates in batteries and supercapacitors.[146] Specifically, NFs have been very useful in the alkaline electrocatalytic study of both HER and HMF oxidation.

When the HER is carried out in alkaline media, nickel (Ni) is a low-cost catalyst and an interesting alternative to platinum. It has been determined that the porosity of nickel foams and the presence of fine nanostructures influence the electrocatalytic activity of HER.[147–149] Furthermore, it has been found that the size of the pores or holes is related to the size of the H_2 bubbles.[150]

It is widely known that HER can proceed through two possible mechanisms,[151] which always include H_2 adsorption (Volmer step) followed by electrochemical desorption (Heyrovsky step) or chemical recombination (Tafel step). When each of these steps is the rate-determining step of HER, a Tafel slope value of 120, 40, or 30 mV dec^{-1}, respectively, is obtained. However, when HER is carried out on a porous matrix, such as nickel foams, deviations in Tafel slope values are often observed, due to the complexity of the 3D structure of the electrodes.[150]

As an example to explain the excellent electrochemical activity of NFs, R. Latsuzbaia *et al.* (2018) carried out a continuous electrochemical HMF oxidation process to FDCA was developed in an alkaline medium on catalyst materials such as Au, Au_3Pd_2, Pt, PbO_2, Ni/NiOOH foam, and graphite.[152] As a result, non-noble Ni/NiOOH electrodes showed better performance compared to noble metal alternatives, reaching FDCA yield of $\approx$90% and faradaic efficiency of $\approx$80%.

Recently, A. Delparish *et al.* (2022) explained the mechanism and reaction kinetics of the electrochemical oxidation of HMF on $Ni(OH)_2$/NiOOH, and its implications in the design of a reactor to carry out this reaction.[153] The reaction was carried out in a parallel plate electrochemical microreactor using Ni plates as working electrode and counter electrode. The work showed the characterization of the mass transfer of the reactor and a detailed parametric study. Almost complete conversion was obtained at pH 13, applying a cell potential of 1.7 V and a short residence time of less than 380 s. The kinetic model of this study suggested that the reaction proceeds through the adsorption of HMF and intermediates on NiOOH, the mechanism of which is explained below.

When performing voltammetric studies in an electrochemical cell, Ni meets the alkaline solution at pH 13, producing $Ni(OH)_2$ on the surface spontaneously:[154]

$$Ni \xrightarrow{OH^-} Ni(OH)_2 \quad (4)$$

Cyclic voltammetry measurements on the $Ni(OH)_2$ covered Ni electrode in presence and absence of HMF usually show an anodic peak followed by a strong current increase due to the oxygen evolution reaction (OER). It should be remembered that

the OER is the main reaction that competes with the oxidation of HMF. The anodic peak is attributed to the oxidation of the $Ni(OH)_2$ sites to NiOOH:[153–155]

$$Ni(OH)_2 + OH^- \underset{k_{-1}}{\overset{k_1}{\rightleftarrows}} NiOOH + H_2O + e^- \quad (5)$$

In the absence of HMF, this current reaches a maximum followed by a valley as the $Ni(OH)_2$ sites are depleted during the sweep, whereas in the presence of HMF, the anodic peak increases its value in current and the trough is contracts. This increase corresponds to the oxidation of HMF on the NiOOH sites.[153] This causes the NiOOH sites to be reduced to $Ni(OH)_2$. In this way, the NiOOH sites become available again to participate in the surface oxidation reaction (eqn (5)), thus contributing to the anodic current. The disappearance of the valley in the presence of HMF (especially when HMF concentrations are higher), suggests that the surface coverage of HMF and/or its oxidation products plays a key role in the electrocatalytic process.[153]

J. Zhang *et al.* (2021) developed an ultrathin nickel hydroxide nanosheets *in situ* on commercial nickel foam ($Ni(OH)_2$/NF) as an anode for the electrocatalytic oxidation of HMF to FDCA, where the complete conversion of HMF was carried out, with a yield of 100% of FDCA and >99% faradaic efficiency applying a potential of 1.39 V (*vs.* RHE) during 90 min of reaction.[99]

Table 2 summarizes the electrocatalytic performance of different electrode materials incorporating NFs, including the system used, HMF concentration, electrolyte, onset potential (*vs.* RHE), FDCA yield and faradaic efficiency (FE).

In addition, given the extraordinary electrocatalytic characteristics of NFs, they are often used as modification substrates, adding other interesting materials to their surface in order to enhance their electrochemical properties towards HER and HMF oxidation[52,101,156–163] which, to facilitate comparison, are also presented in Table 2.

4.2 Noble metals

Almost two decades after the first investigation on the electrochemical oxidation of HMF carried out in 1991, a new electrochemical investigation was carried out by K. R. Vuyyuru (2012) where the effect of the pH of the reaction medium and the electrocatalyst on the electrochemical oxidation of HMF was analyzed.[164] In this study it was reported that in the absence of a catalyst, HMF was not very stable under strongly alkaline conditions (*i.e.*, pH > 13). When a Pt electrode was used at pH 10, about 70% conversion of HMF was obtained at a current density of 0.44 mA cm^{-2}. However, only the DFF intermediate was obtained in 18% yield and the amount of FDCA was <1%. Apparently, Pt is not a suitable electrocatalyst for HMF oxidation, at least under these working conditions.

Electrocatalysts that include a single noble metal such as Pd,[165,166] Pt,[91,152] Au,[165] and Ru,[167,168] have been studied in the electrooxidation of alcohols, aldehydes and furans as they have shown outstanding capabilities in the activation of molecular oxygen.[169,170] However, these noble metals have disadvantages in the electrocatalytic oxidation of HMF, obtaining unfavorable yields.[171] This is because HMF carbonyl groups usually occupy the surface sites of metals through intense adsorption, which causes electrocatalyst deactivation.[172] In addition, it has been found that despite the fact that noble metal electrocatalysts lead to obtaining low onset potentials, the supplied current density is considerably low, which hinders their application in the electrocatalytic oxidation of HMF.[89,171]

According to this, D. J. Chedderdon *et al.* (2014) addressed the electrochemical oxidation of HMF using noble metals including Au and Pd and their alloys.[165] In this study, the comparison of the oxidation of HMF, 5-hydroxymethyl-2-furancarboxylic acid (HMFCA) and 2-formyl-5-furancarboxylic acid (FFCA) on Au and Pd led to the conclusion of that Au was considerably more efficient than Pd for the oxidation of the aldehyde group in HMF. In addition, the bimetallic Au/Pd electrodes presented higher electrocatalytic activity compared to each metal individually. It was further found that alloying Au with Pd enhanced its activity towards oxidation of the hydroxymethyl group in HMFCA. In addition, the bimetallic $PdAu_2$/C system significantly improved the efficiency of the electrochemical oxidation of HMF, achieving a complete conversion of HMF, where the yield of FDCA formation at a potential of 0.9 V (*vs.* RHE) was 83%. However, this electrocatalytic methodology

Table 2 Electrocatalytic performance of different electrode materials using nickel foams on the electrooxidation of HMF towards FDCA

System	[HMF]	Electrolyte	E_{onset}, V *vs.* RHE	FDCA yield	FE	Ref.
Ni/NiOOH	10 wt%	0.1 M Na_2SO_4 + additions of NaOH to maintain, pH = 12	—	∼90%	∼80%	152
$Ni(OH)_2$/NiOOH	20 mM	KOH and Na_2SO_4, pH = 13	1.7	52% max.	—	153
$Ni(OH)_2$/NF	10 mM	1 M KOH	1.39	100%	>99%	99
β-$Co_{0.1}Ni_{0.9}(OH)_2$/NF	50 mM	1 M KOH	∼1.3	—	∼93%	156
Ni_2P/NF	10 mM	1 M KOH	1.423	—	98%	52
Ni_xSe_y–NiFe@NF	10 mM	1 M KOH	∼1.37	99.3%	98.9%	157
Ni_xB/NF	10 mM	1 M KOH	1.45	98.5%	∼100%	158
NiB_x@NF	10 mM	1 M KOH	1.7	—	≥99%	101
δ-MnO_2/NF	10 mM	1 M KOH	1.35	98%	98%	159
$NiCo_2O_4$ nanowires/NF	10 mM	0.1 M KOH	1.55	90%	∼100%	160
$NiCo_2O_4$/NF	5 mM	1 M KOH	1.5	—	87.5%	161
$CuCo_2O_4$/NF	50 mM	1 M KOH	1.23	93.7%	94%	162
N–Co_3O_4/NF	50 mM	1 M KOH	1.38	96.4%	99.5%	163

generated other reaction intermediates (mainly HFCA), which hinders the purification process of FDCA from the electrolyte. In the context of these results, many studies have revealed that Au is more efficient for the selective oxidation of aldehyde groups; however, this noble metal can be deactivated by the organic products formed.[173,174]

In contrast, Pt and Pd are more efficient for the oxidation of alcohol groups and stabilize Au.[175,176] For this reason, AuPd alloys exhibit great stability and high yields in HMF oxidation.[165,166,171,177] given its remarkable ability to oxidize aldehyde and alcohol groups of HMF.[171] Attempts have been made to continue using noble metals in improving the electrochemical activity of other materials in the electrooxidation of HMF, such as using sputter-coated glass with Au on Ti[178] where, despite the fact that the oxidation of HMF to FDCA was carried out at an overpotential of 1.54 V, the performance of FDCA and the faradaic efficiency were increased to values over 99%.

C. Zhou *et al.* (2019) prepared Fe_3O_4 decorated reduced graphene oxide supporting platinum nanocatalyst (Pt/Fe_3O_4/rGO) and applied it in the electrooxidation of HMF to produce FDCA.[179] The results showed that the introduction of Fe_3O_4 increases the utilization of platinum, the catalytic activity and the recycling property of the catalyst. It was also shown that the dispersion of Pt increased about 10% when decorating with Fe_3O_4 given the electrochemical active and chemical adsorption surface area. The Pt/Fe_3O_4/rGO system presented better activity compared to Pt/rGO and achieved a conversion of 100% of HMF and a yield higher than 98% of FDCA in 0.1 M K_2SO_4 aqueous solution, after 8 h under mild conditions.

A. R. Poerwoprajitno *et al.* (2020) synthesized branched gold-supported nickel nanoparticles (Ni/Au-br-NPs) to carry out the anodic oxidation of HMF.[180] In this work we highlight a cubic core hexagonal branching growth mechanism that allows the formation of branched Ni nanoparticles with adjustable branch length. Ni branches grew on Au nanoparticles. Branched Ni nanoparticles had higher activity in the anodic oxidation of HMF than spherical amorphous Ni nanoparticles. This attractive performance is attributed to the large surface area and exposure of surface facets along the Ni branches. This work is a new example that the presence of noble metals would not directly help in the electrocatalytic oxidation of HMF. However, noble metals can be quite useful in the construction of electrocatalysts to improve the electrocatalytic activity and efficiency of other non-noble metals.

The electrocatalytic performance of different electrode materials incorporating noble metals presented above is summarized in Table 3.

4.3 Non-noble metals

Given the high economic cost of noble metals, many research groups have focused on manufacturing new electrocatalysts based on non-noble metals, in order to reduce the production costs of both H_2 and FDCA. Transition metal are widely used as electrocatalysts due to various electronic configurations of 3d orbital.[181]

One of the requirements for an electrocatalyst to be widely applicable is to have a high abundance in the earth's crust. The most abundant 3d metal is iron, which, by presenting multiple possible oxidation states, has been applied in multiple ways in chemocatalytic processes. However, $Fe^{III}O_xH_y$ presents low conductivity, limiting its applicability for electrocatalytic oxidation reactions.

J. N. Hausmann *et al.* (2021) showed that iron incorporated into the conductive intermetallic iron silicide (FeSi) can be a good alternative as a more conductive material.[182] Unlike low-Si Fe and Si alloys, intermetallic FeSi exhibits an ordered bonded structure that includes covalent and ionic contributions along with conducting electrons to mediate the selective oxidation of HMF to FDCA. It was shown that, under the applied corrosive alkaline conditions, FeSi partially forms a single iron(III) oxide phase [FeO_6] consisting of octahedrons sharing edges and corners together with oxidized silicon species. The FeSi electrocatalyst achieved 94% faradaic efficiency for the production of FDCA from HMF at an electrochemical potential less than 1.35 V (*vs.* RHE).

Recently, X. Pang *et al.* (2022) worked on the application of copper-based electrocatalysts.[183] In this work, Cu foam decorated with $Cu(OH)_2$ (CF–$Cu(OH)_2$) was successfully fabricated as an efficient catalyst, and CuOOH active species generated by electrochemistry were demonstrated as the main catalytic sites for HMF oxidation. The CF–$Cu(OH)_2$ catalytic sites for HMF oxidation were mainly attributed to the surface active CuOOH species. During the electrocatalysis of 100 mM HMF a high FDCA yield of 98.7% was obtained, while the conversion of HMF and FE were close to 100%.

F. Kong *et al.* (2021) synthesized a flowerlike hybrid composed of sulfur-modulated metallic nickel nanoparticles coupled with carbon frameworks (S–Ni@C) *via* two steps, achieving high selectivity and efficiency for HMF oxidation.[184] Lignosulfonate, which is pulp waste, was used as a carbon and sulfur precursor. Surface nickel hydroxide species and carbon shells contributed to the improved electroactivity. As a result, the optimized S–Ni@C electrode exhibited a nearly 100% conversion of HMF, 96% yield of FDCA, and 96% faradaic efficiency.

Additionally, it has been common to design and manufacture bifunctional electrocatalyst materials for the simultaneous production of H_2 and FDCA from bi- or tri-metallic alloys. Alloys can contain intermetallic interactions in the form of ionic, covalent, and metallic bonds.[185] The covalent interactions of the individual phases allow the intermetallic compound to possess a more ordered crystalline structure, forming a new scaffold-like organization of the electronic structure. This organization presents the ability to facilitate the processes of transfer and adsorption of electrons.[186] In this way, depending on the alloying strategy, a combination of specific properties of each metallic component can be achieved, which counteracts the weaknesses of monometallic catalysts,[171] which improves both the HER reduction process and the electrochemical oxidation of HMF.

In the search for new and attractive possibilities, M. Cai *et al.* (2020) studied the electrooxidation of HMF in FDCA using Ni-based two-dimensional metal–organic frameworks (2D MOFs) as electrocatalysts.[187] The as-prepared Co-doped 2D MOFs

Table 3 Electrocatalytic performance of different electrode materials using noble metals on the electrooxidation of HMF towards FDCA

System	[HMF]	Electrolyte	E_{onset}, V *vs.* RHE	FDCA yield	FE	Ref.
$PdAu_2$/C	20 mM	0.1 M KOH	0.9	83%	—	165
Sputter-coated glass with Au on Ti	5 mM	0.5 M borate buffer, pH = 9.2	1.54	>99%	>99%	178
Pt/Fe_3O_4/rGO	25 mM	0.1 M K_2SO_4	—	98%	—	179
Ni/Au-br-NPs	10 mM	0.1 M KOH	1.43	—	—	180

NiCoBDC (Ni^{2+}, BDC = terephthalic acid) have a FDCA yield of 99% and a faradaic efficiency of 78.8% at 1.55 V (*vs.* RHE), as performed in an electrolyte at pH 13. Due to the accessible pores of HMF molecules, abundant exposed active sites and coupling effects between Ni and Co atoms, 2D NiCo-MOFs realized an interesting electrocatalytic activity and robust electrochemical durability.

In a similar study, X. Deng *et al.* (2022) carried out the simultaneous electrochemical production of FDCA and H_2 *via* bifunctional copper sulfide nanowire@NiCo-layered double hydroxide (Cu_xS@NiCo-LDH) core–shell nanoarray electrocatalysts.[188] Due to the Co/Ni interaction in the LDH nanosheet layer, the fast charge transfer induced by the Cu_xS core, and the open nanowire@nanosheet structure, the electrocatalysts exhibit an attractive onset potential of 1.3 V (*vs.* RHE) for HMF oxidation with faradaic efficiency towards FDCA and H_2 is close to 100%. Also, the bifunctional two-electrode electrolyzer requires a voltage of 1.34 V to co-generate H_2 and FDCA at 10 mA cm^{-2}.

Co and Ni alloys were also studied by W. Chen *et al.* (2020), who pointed out that for β-$Ni(OH)_2$ and NiO, the origins of oxidation of nucleophiles such as HMF are the β-Ni(OH)O and NiO(OH) containing oxygen-containing species of electrophilic lattice and electrophilic adsorption oxygen, respectively.[156] In this study it was proposed that the electrocatalytic performance of β-$Ni(OH)_2$ can be remarkably regulated by adjusting the oxygen ligand environment of the lattice through Co(II) incorporation. The electrocatalyst synthesized in this study (β-$Co_{0.1}Ni_{0.9}(OH)_2$/NF), exhibited outstanding electrocatalytic activities in the oxidation of various nucleophiles. Specifically, in the electrooxidation of HMF, β-$Co_{0.1}Ni_{0.9}(OH)_2$/NF, managed to carry out the electrochemical conversion at a potential close to 1.3 V (*vs.* RHE), with a faradaic efficiency of around 93%.

It is interesting to note that Ni usually offers high currents, while Co reduces the onset potential.[189,190] Consequently, NiCo alloys achieve low onset potential and large catalytic currents, which increases HMF oxidation efficiency.[171,191] As an example, R. Zheng *et al.* (2021) constructed a hierarchically structured NiCo–Cu-based electrocatalyst for integrated H_2 evolution and HMF oxidation in alkaline conditions.[191] The electrocatalyst consists of Cu nanowire arrays grown on a three-dimensional Cu foam substrate modified by nickel–cobalt layered double hydroxide nanosheets ($NiCo_{NSs}/Cu_{NWs}$). When HMF oxidation and H_2 evolution are integrated into a two-electrode electrolyzer with the $NiCo_{NSs}/Cu_{NWs}$ electrocatalyst couple, the potential required to achieve a current density of 10 mA cm^{-2} is 1.44 V, approximately 250 mV lower than that of overall water splitting. Also, it was reported that HMF oxidation occurs upon the formation of Ni^{3+} species, leading to earlier catalytic onset (around 300 mV ahead) in comparison with the OER triggered by the higher-oxidation-state Ni^{4+} species.

In another study, W.-J. Liu *et al.* (2018) investigated the development of NiFe layered double hydroxide (LDH) bimetallic nanosheets on carbon fiber paper as anode for the electrochemical oxidation of a highly concentrated solution of HMF to FDCA.[105] A near-quantitative yield of FDCA and 99.4% faradaic efficiency of HMF conversion under ambient conditions were achieved during the electrochemical process. Also, HMF has a higher rate of oxidation than water, so the bimetallic electrocatalyst is a good alternative as a bifunctional material towards both HMF and HER oxidation in an alkaline medium.

In addition, M. Zhang *et al.* (2020) developed trimetallic NiCoFe-layered double hydroxides nanosheets (NiCoFe-LDHs) for efficient for O_2 evolution and selective oxidation of HMF.[192] For comparison, two sets of bimetallic NiCo- and NiFe-LDHs were similarly synthesized and evaluated. The trimetallic NiCoFe-LDHs nanosheets reached a durability of more than 10 h, much better than that of NiCo- and NiFe-LDHs. The trimetallic electrocatalyst also exhibited an overpotential of 280 mV to achieve 20 mA cm^{-2}. The conversion of HMF was 95.5% and the yield of FDCA obtained in 1 h was 84.9%.

Anagously, X. J. Bai *et al.* (2021) prepared a ternary Metal–Organic Framework (MOF) nanoarray that was hydrothermally deposited on Ni foam *via* assembling of Co^{2+}, Ni^{2+} and Fe^{2+}.[193] The integrated MOF composite (NiCoFe-MOFs) can directly act as an electrode, which exhibits electrocatalytic HMF oxidation activity with a potential of 1.35 V (*vs.* RHE). It was indicated that the electrocatalytic performance for HMF oxidation is attributed to the abundant accessible active sites of two-dimensional morphology and the optimized electronic structure of the intrinsic catalytic centers in MOFs. The constant potential electrolysis at 1.4 V (*vs.* RHE) in combination with chromatographic analysis reveals a high faradaic efficiency close to 100% towards the production of FDCA with a yield of 99.76%.

In addition to the cases discussed above, it has been found that for those alloy electrocatalysts made up of readily available transition metals such as Mn, Fe, Co, Ni, Cu, Mo, the d-band center of the electrocatalysts is considered as an important descriptor when evaluating the electrocatalytic efficiency of materials. In this context, the center of the d band plays an important role during chemisorption. It has been determined that the closer the d-band center and the Fermi energy level are, the higher the adsorption energy. Therefore, this closeness implies that the strength of the

interaction between the reaction substrate and the electrocatalyst is stronger.[171,194–196]

As an example, S. Li *et al.* (2019) worked on the restructuring of the d-band center of the VN alloy so that the d-band center of V as the active species was closer to the Fermi energy level compared to the conventional V_2O_5 catalyst, to improve the interaction between VN and HMF.[197] The alloy strategy allowed to facilitate the adsorption of HMF with VN and improved the activity of the oxidation reaction, with a conversion of HMF of 99%, yield of FDCA of 97% and faradaic efficiency of 86%. Specifically, the adsorption of HMF with VN occurred on two functional groups, the aldehyde group (–CHO) and the hydroxymethyl group (–CH_2OH), while when HMF adsorbed on the surface of V_2O_5, only the aldehyde group was adsorbed. (–CHO), and the adsorption energy was lower than the adsorption energy on VN. Theoretical calculations revealed that the higher performance of VN for the electrocatalytic production of FDCA can be attributed to its lower d-band center level relative to the Fermi level compared to that of V_2O_5, which favors HMF chemisorption and activation.

Table 4 below shows the electrocatalytic performance of different electrode materials using non-noble metals discussed above.

4.4 Metal non-oxides

Metal non-oxides such as phosphides,[140,198,199] selenides,[157,200,201] nitrides[197,202] and borides[158,203] have been used successfully as efficient electrocatalysts for the conversion of HMF to FDCA.

N. Jiang *et al.* (2016) electrodeposited cobalt phosphide (Co–P) on copper foam (Co–P/CF) as a competent electrocatalyst for co-production of FDCA at the anode and H_2 at the cathode simultaneously in alkaline medium.[140] In this work, Co–P required a current density of 20 mA cm^{-2} for the oxidation of HMF in 1.0 M KOH with 50 mM HMF at 1.38 V (*vs.* RHE), before the onset of O_2 evolution as competition reaction. Chronoamperometry showed almost complete conversion of HMF and a yield close to 90% of FDCA at ambient conditions (1 atm and room temperature). Regarding its performance as a bifunctional material, by integrating HMF oxidation and H_2 evolution in an electrolyser with a Co–P/Co–P catalyst pair, the potential required to achieve a current density of 20 mA cm^{-2} was 1.44 V, 150 mV, which is lower than water in general. Co–P was able to catalyze the evolution of H_2 as the cathode reaction with a faradaic efficiency of 100%.

Recently, in a similar work M. J. Kang (2022) prepared Deep Eutectic Solvent (DES) stabilised Co–P films as efficient and durable catalytic electrodes for HMF oxidation using 0.5 M $NaHCO_3$ (pH 12) solution as the electrolyte during the electrochemical process.[199] Experimentally, electrodeposition of Co–P on Cu foam was performed in different solvents of water and DES. Co–P synthesized in DES solvent showed 99% HMF conversion with 85.3% FDCA yield, a considerably higher yield compared to Co–P synthesized under H_2O as solvent. It also showed long-term stability. DES solvent has advantages such as good ionic conductivity, easy preparation, non-toxic, low cost and biodegradable. In this context, this work suggests the usability of DES to replace water as a reaction solvent to prepare electrodes by electrodeposition, showing high stability, sustainability, and better electrode efficiency.

Likewise, nickel phosphides have attracted increasing attention due to their exclusives structures and electronic properties.[204] Nickel phosphide electrocatalysts on nickel foam (Ni_2P/NF)[52] have been shown to be useful in the production of H_2 and FDCA with faradaic efficiencies of 100% and 98% respectively. In the same way, a phosphorus-containing deep eutectic liquid precursor was recently developed. M. Xing *et al.* (2023) obtained 3D cobalt-doped self-supporting $Ni_{12}P_5/Ni_3P$ nanowire networks coated with a thin layer of carbon (Co–Ni_xP@C) by pyrolysis method.[198] In this research it was revealed that Co-doping in Ni_xP@C can promote the adsorption and activation of 5-hydroxymethylfurfural (HMF) molecules and optimize the H* absorption energy barrier. Co–Ni_xP@C was used as an efficient bifunctional electrocatalyst for HMF oxidation in conjunction with HER in 1.0 M KOH solution. Nearly 100% yield of FDCA was achieved. The self-sufficient electrocatalyst showed high activity and stability for both HER and HMF conversion. Besides, the oxidation of HMF together with HER can be efficiently driven by a commercial 1.5 V photovoltaic panel under sunlight, demonstrating the obtaining of green products.

Table 4 Electrocatalytic performance of different electrode materials using non-noble metals on the electrooxidation of HMF towards FDCA

System	[HMF]	Electrolyte	E_{onset}, V *vs.* RHE	FDCA yield	FE	Ref.
FeSi		1 M KOH	<1.35	—	94%	182
CF–$Cu(OH)_2$	100 mM	1 M KOH	—	98.7%	~100%	183
S–Ni@C	10 mM	1 M KOH	1.35	96%	96%	184
NiCo-MOF	10 mM	0.1 M KOH	1.55	99%	78.8%	187
Cu_xS@NiCo-LDH	10 mM	1 M KOH	1.3	99%	99%	188
β-$Co_{0.1}Ni_{0.9}(OH)_2$/NF	50 mM	1 M KOH	~1.3	—	~93%	156
$NiCo_{NSs}/Cu_{NWs}$	10 mM	1 M KOH	1.44	~100%	—	191
NiFe-LDH	100 mM	1.0 M KOH	1.32	98%	99.4%	105
NiCoFe-LDHs	10 mM	1 M NaOH	1.54	84.9%	90%	192
NiCoFe-MOFs	10 mM	1 M KOH	1.4	99.76%	~100%	193
VN	10 mM	1 M KOH	1.36	97%	86%	197
VN coupled with Pd/Vn	10 mM	1 M KOH	1.36	89%	—	197

Iron phosphides have also been studied as HMF electrocatalysts. For example, G. Yang *et al.* (2020) developed a porous nanospindle composed of carbon-encapsulated MoO_2–FeP heterojunction (MoO_2–FeP@C) as a robust bifunctional electrocatalyst for coupled HER and HMF electrooxidation.[104] by X-ray photoelectron spectroscopy analysis and theoretical calculations the electron transfer from MoO_2 to FeP at the interfaces was confirmed. Thus, the accumulation of electrons in FeP favors the absorption of H_2O and H* for HER, while the accumulation of holes in MoO_2 is responsible for improving the electrooxidation of HMF.

This electrocatalyst showed HMF conversion of almost 100% and FDCA was obtained with the selectivity of 98.6%. The electrolyzer that uses MoO_2–FeP@C for cathodic H_2 and anodic FDCA production required a voltage of 1.486 V at 10 mA cm^{-2} and can be powered by a solar cell (considering output voltage: 1.45 V).

Some metal selenides have also been used for efficient electrocatalytic H_2 and HMF production. C. Yang *et al.* (2021) analyzed the performance of Ni_xSe_y-based electrocatalysts, focusing on both the electronic properties and the intrinsic characteristics of the components of the possible Ni_xSe_y structures.[205] In the various structures of Ni_xSe_y, nickel has a unique valence electron configuration ($3d^84s^2$) and is the main site of catalytic activity. On the other hand, Se in Ni_xSe_y not only presents the same valence electrons and oxidation number than S and O but also has excellent intrinsic metal properties, which causes better electrical conductivity as well as electrocatalytic activity. Together Ni and Se could form stoichiometric compounds (NiSe, $NiSe_2$, Ni_3Se_2, Ni_3Se_4) and nonstoichiometric compounds ($Ni_{0.85}Se$), which may be due to the electronegativity difference between Ni (1.9) and Se (2.4). C. Liu *et al.* (2018) determined that d-band state of NiSe is equivalent to that of platinum, showing excellent electrochemical activity for HER.[206] For this reason, Y. Huang *et al.* studied the electrooxidation of primary amine to replace OER for enhancing HER using NiSe nanorod arrays.[207] A mechanistic analysis indicated that the Ni^{II}/Ni^{III} redox couple could serve as the active species for the transformation of primary amines.

Y. Zhong *et al.* (2022) reported Grass-like Ni_xSe_y nanowire arrays shelled with NiFe LDH nanosheets as a 3D hierarchical core–shell electrocatalyst for efficient upgrading of HMF.[157] In this work, Ni_xSe_y–NiFe was grown on Ni foam (Ni_xSe_y–NiFe@NF) for efficient electrocatalytic production of FDCA. In view of the electrical conductivity and good mechanical strength of the Ni_xSe_y nanowire core, abundant exposed active sites of the NiFe LDH nanosheet shell, and the open structure of the hierarchical nanoarrays, the integrated core–shell Ni_xSe_y–NiFe LDH@NF electrode exhibited outstanding catalytic performance for HMF oxidation. The electrocatalyst presented FDCA yield of 99.3% with faradaic efficiency of 98.9% and superior stability retaining 96.7% FE after six successive electrolysis cycles.

Similarly, in another research L. Gao *et al.* (2020) used NiSe@NiO_x core–shell nanowires to effectively upgrade HMF to FDCA.[201] The NiSe@NiO_x features conductive NiSe nanowires as a core and active NiO_x as a shell, showing a near-quantitative yield of FDCA and 99% faradaic efficiency. It was revealed by X-ray photoelectron spectroscopy that the high valence of Ni species in the NiO_x shell may act as active sites. Further integrated electrolyzer can produce FDCA and H_2 simultaneously, with a 100% of faradaic efficiency after six successive cycles.

A work was carried out by X. Huang *et al.* (2020) in which the union of Co and Se was studied. Here, it was found that the electrocatalytic performance of cobalt oxide (CoO) could be considerably improved by means of doping with Se for the electrooxidation of HMF to FDCA.[200] The resulting CoO–$CoSe_2$ with a CoO/$CoSe_2$ molar ratio of 23 : 1 showed high stability to produce FDCA with yield of 99% and a faradaic efficiency of 97.9% at a potential of 1.43 V (*vs.* RHE). This study indicates that the introduction of Se can improve the catalytic activity and the selectivity to FDCA, due to the increase in electrochemical surface area and the reduction of the charge transfer resistance.

Some investigations have shown interesting results when incorporating metal nitrides. For example, in the research of Li *et al.* (2019) above discussed[197] in which FDCA was produced from electrochemical oxidation of HMF using VN, with FDCA yield of 97% and faradaic efficiency of 86%. In a complementary way, N. Zhang *et al.* (2019) studied the electrochemical oxidation of HMF and HER on nickel nitride/carbon nanosheets (Ni_3N@C).[202] Ni_3N@C electrode showed a potential of 1.38 V at current density of 50 mA cm^{-2}, and the yield of the oxidation product FDCA remained at 98% after six cycles of electrolysis with the same surface. The overpotential of the dual-electrode electrolyzer in simultaneous production of FDCA and H_2 is reduced by at least 240 mV replacing HMF oxidation by OER. Moreover, it also shows efficient electrooxidation performance for other biomass substrates. It provides an interesting strategy to improve the electrochemical activity of the bifunctional catalyst for both biomass conversion and H_2 production.

Regarding the use of metal borides, several works have demonstrated their applicability in the electrocatalysis of HMF. X. Song *et al.* (2020) doped nickel borides (NiB_x) with different amounts of phosphorus were prepared and applied to the electrocatalytic conversion of HMF.[203] It was found that the FDCA yield on P-doped NiB_x (NiB_x–P_y) changed with the increase of phosphorus content (first gradually increased and then decreased). When NiB_x–$P_{0.07}$ ($n_P/n_{Ni} = 0.07$) was used as electrode, the FDCA yield reached a maximum of 90.6% and faradaic efficiency of 92.5% at 1.464 V (*vs.* RHE). XPS analysis indicated that the P dopant caused relative displacement of electrons from surface nickel. Thus, nickel hydroxide species increased, which improves the electrocatalytic performance towards FDCA production. Besides, appropriate phosphorus doping accelerated charge transmission capability of NiB_x–P_y improving the electroactivity.

The electrooxidation of HMF to FDCA was also reported by S. Barwe *et al.* (2018) using high surface area nickel boride modified Ni foam (Ni_xB) as electrode.[158] The electrolysis was carried out at constant potential and HPLC studies revealed a faradaic efficiency close to 100% in the production of FDCA and a yield of 98.5%. Electrochemical test coupled with ATR-IR spectroscopy, in agreement with HPLC analysis, showed that

HMF is preferentially oxidized through 5-hydroxymethyl-2-furancarboxylic acid rather than through 2,5-diformylfuran.

P. Zhang *et al.* (2019) reported that NiB_x electrocatalyst presents excellent selectivity, conversion and faradaic efficiency values both at the cathode and at the anode simultaneously using water as O_2 and H_2 source.[101] A conversion efficiency and selectivity of ≥99% was observed during the oxygenation of HMF to FDCA and the simultaneous hydrogenation of *p*-nitrophenol to *p*-aminophenol. This paired electrosynthesis cell has also been coupled to a solar cell as an independent reactor in response to sunlight. The electrocatalytic performance of electrode materials using metal non-oxides is presented in Table 5.

4.5 Metal oxides and spinel oxides

Metal oxides have great importance in various electrochemical processes due to their ability to generate charge carriers when activated with the required amount of energy. The charge transport characteristics, the electronic structure and the light absorption properties of most metal oxides have made possible their application in both catalytic and photocatalytic processes.[208] Transition metal oxides are widely used as electrocatalyst or electrocatalyst support. Due to various electronic configurations of 3d orbital, such oxides usually show tunable acidity–basicity, redox property, crystal defects and diverse oxygen species, depending on the ratios of different components.[181]

S. R. Kubota *et al.* (2018) carried out the electrochemical oxidation of HMF in acidic media by using a manganese oxide (MnO_x) anode to remove the need to vary the pH to separate FDCA.[91] The MnO_x electrocatalyst achived a FDCA yield of 53.8% in a pH 1 H_2SO_4 solution, in which FDCA precipitation occurred spontaneously from the reaction acidic solution. In contrast, Ch. Wang *et al.* (2022) reported synthesize mesoporous δ-MnO_2 on nickel foam (δ-MnO_2/NF) for FDCA production in alkaline media.[159] By taking structural advantages of mesoporous oxides, this mesoporous δ-MnO_2 is employed as a highly efficient, selective, HMF electrochemical oxidation to FDCA with higher yield (98%) and a faradaic efficiency of 98%.

Furthermore, it is possible to combine chemical properties of different metal oxides to mediate the electrochemical oxidation of HMF under certain conditions. As an example, L. Gao *et al.* (2020) carried out the electrochemical conversion of HMF using a TiO_x@MnO_x electrocatalyst in order to obtain FDCA precipitation in one step in acidic media.[209] The TiO_x@MnO_x electrocatalyst with the active MnO_x species was confined on the TiO_x. In the successive conversion of 100 mM HMF, the yield of the FDCA precipitate was close to 24%. Electrolysis under various conditions revealed that the electrolyzer, the electrolysis potential and temperature, and the HMF concentration are decisive in the performance of FDCA. It was determined that the conversion yield of HMF is specifically due to the activity of the metal oxide MnO_x for the oxidation of HMF and the resistance to acidic medium presented by the TiO_x nanowire structure.

Transition metal oxides with different compositions and morphologies are compounds of great importance in the electro-oxidation of biomass and biomass derivatives. Specifically, materials based on transition metals such as Fe, Co, Ni and Cu have been the focus of research due to their low cost, exceptional efficiency, good selectivity, and stability. Nickel is one of the most widely used metallic materials as an anode for the electro-oxidation of biomass and biomass derivatives in alkaline solution.[210]

In this context, F. J. Holzhäuser *et al.* (2020) performed the electrocatalytic oxidation of HMF into FDCA in alkaline aqueous solutions using commercial nickel oxide (NiO) or a mesostructured nickel oxide derived by CMK-1 templating (NiO-CMK-1).[211] The authors noted that electrocatalytic activity and selectivity of FDCA were highly dependent on the electrocatalyst structure. NiO-CMK-1 facilitates multiple times higher FDCA selectivity (>80%) compared with commercial NiO (30%). The exposed material surface and structure of the electrocatalysts were studied by nitrogen physisorption and powder X-ray diffraction revealing that both NiO and NiO-CMK-1 possess a face-centered cubic crystal structure but distinctly different exposed surface areas. Since NiO-CMK-1 enables remarkably improved catalytic activity for the oxidation of HMF, a recycling study was conducted with five consecutive catalytic cycles emphasizing the technological potential of this approach. As a result, it could be shown that the advantages of structured

Table 5 Electrocatalytic performance of different electrode materials using metal non-oxides on the electrooxidation of HMF towards FDCA

System	[HMF]	Electrolyte	E_{onset}, V *vs.* RHE	FDCA yield	FE	Ref.
Co–P/CF	50 mM	1 M KOH	1.38	∼90%	100%	140
Co–P	5 mM	0.5 M $NaHCO_3$	1.34	85.3%	77.3%	199
Ni_2P/NF	10 mM	1 M KOH	1.423	—	98%	52
Co–Ni_xP@C	10 mM	1 M KOH	1.5	∼100%	96.8	198
MoO_2–FeP@C	10 mM	1 M KOH	1.359	99.4%	97.8%	104
Ni_xSe_y–NiFe@NF	10 mM	1 M KOH	∼1.37	99.3%	98.9%	157
NiSe@NiO_x	10 mM	0.1 M KOH	1.423	99%	99%	201
CoO–$CoSe_2$	10 mM	0.1 M KOH	1.43	99%	97.9%	200
Ni_3N@C	10 mM	0.1 M KOH	1.38	98%	>99%	202
NiB_x–$P_{0.07}$	10 mM	0.1 M KOH	1.464	90.6%	92.5%	203
Ni_xB/NF	10 mM	1 M KOH	1.45	98.5%	∼100%	158
NiB_x@NF	10 mM	1 M KOH	1.7	—	≥99%	101

mesoporous NiO over bulk NiO as base material and the importance of surface enlargement in the electrochemical oxidation of HMF. An HMF conversion of 65% was achieved with FDCA selectivity of 79% and a total product selectivity of approximately 100%.

Other metallic components are often introduced to prepare bimetallic electrocatalysts showing attractive results, due to the synergistic effect between different metals as in the case of spinel oxides. Spinel oxides are metal oxides with the chemical formula AB_2O_4 and a face-centered cubic crystal structure. The spinel structure presents tetrahedral coordination for divalent cations (A^{2+}) and octahedral coordination for trivalent cations (B^{3+}).[212–214] Compounds with a spinel-like structure, possessing transition metal ions, have a large number of technological applications due to their structural, electrical and magnetic properties.[215] Spinel-type mixed metal oxides have the property of being catalytic materials because they have compact structures where metal cations can occupy octahedral or tetrahedral positions found on the very surface of the catalyst.

Considering Ni and Co based metal oxides, L. Gao *et al.* (2018) reported hierarchical electrocatalysts of $Ni_xCo_{3-x}O_4$ growing vertically on NF.[160] The electrocatalysts were fabricated through a low-temperature hydrothermal method. Their structures were controlled from nanosheets to nanowires by adjusting the Ni/Co ratio. It was reported that all the $Ni_xCo_{3-x}O_4$/NF samples exhibited activity towards the oxidation of HMF, and also the incorporation of Co considerably improved the activity of the materials. Among the synthesized nanostructures, $NiCo_2O_4$ nanowires presented the best performance in terms of onset potential and current density. $NiCo_2O_4$ showed a 90% FDCA yield and almost 100% faradaic efficiency.

Analogously the activity of the Co_3O_4 and $NiCo_2O_4$ electrode with filamentous nanoarchitecture was reported by M. J. Kang *et al.* (2019), which grew on NF using a hydrothermal method.[161] During the electrochemical oxidation of HMF, the role of Co^{3+} in the spinel structure of Co_3O_4 and $NiCo_2O_4$ was investigated. In this report, the filamentous $NiCo_2O_4$ nanostructure showed a conversion efficiency from HMF to FDCA of 99.6% with a selectivity of 90.8%. Additionally, the electrocatalyst was successfully recycled up to three times, retaining more than 80% of the FDCA conversion efficiency.

With the same approach, Y. Lu *et al.* (2020) worked on the exploration of optimal geometrical site in Co_3O_4 for electrochemical HMF oxidation. Co_3O_4 spinel oxide has mixed valences in the presence of both Co^{2+} and Co^{3+}. Identification of the role of each spinel oxide active site is essential to continue designing and producing efficient electrocatalysts for the coproduction of H_2 and FDCA. In this work was analyzed the electrochemical performance of HMF oxidation on cobalt spinel oxides (Co_3O_4, $ZnCo_2O_4$ and $CoAl_2O_4$) by building specific blocks at the tetrahedral site (Co_{Td}^{2+}) and the octahedral site (Co_{Oh}^{3+}) in order to discover the locus dependence and then design an improved electrocatalyst by appropriately regulating each locus.[162] It was found that the electrochemical performance follows the trend: $CoAl_2O_4$ < $ZnCo_2O_4$ < Co_3O_4. It is interesting to note that, according to the theoretical calculations of X. C. Huang *et al.* (2019),[216] the E_g values (band gap) of the three oxides under study are ordered according to Co_3O_4 (0.2–1.9 eV) < $ZnCo_2O_4$ (0.6–2.2 eV) < $CoAl_2O_4$ (0.8–3.6 eV). This trend is inversely proportional to its electrochemical performance towards the production of FDCA, which suggests that, as expected, a smaller energy gap of the semiconductor would produce a decrease in the overpotential required to carry out the electrochemical reaction. The better activity on pure Co_3O_4 than $ZnCo_2O_4$ indicates that both the tetrahedral and octahedral sites in Co_3O_4 contribute to the overall activity but in different ways. In this way, it was found that Co_{Td}^{2+} in Co_3O_4 has the ability to carry out the chemical adsorption of acidic organic molecules, while Co_{Oh}^{3+} performs the function of carrying out the oxidation of HMF. Based on these results, Cu^{2+} was introduced into the spinel oxides to enhance the exposure of Co^{3+}. Finally, the HMF electro-oxidation reaction on the $CuCo_2O_4$ electrode required a potential of 1.23 V, considerably less than Co_3O_4 (1.30 V) and CuO (1.41 V). Besides, with the use of $CuCo_2O_4$ electrode a high yield of 93.7% and faradaic efficiency of 94% were obtained for FDCA production. Table 6 below summarizes the electrocatalytic performance of electrode materials incorporating metal oxides and spinel oxides discussed above.

4.6 Oxygen vacancies

Oxygen vacancies are common defects in metal oxides and play a crucial role in modulating their properties. The introduction of oxygen vacancies is an attractive approach to tune electronic structure and charge transport, generate surface active secondary phases, and modify surface adsorption/desorption behavior between certain reaction intermediates and the electrocatalyst by improving electrocatalytic activity.[217]

Generally speaking, by introducing oxygen vacancies, the bandgap narrows and new states are formed within the bandgap near the Fermi level.[217] A narrower energy gap between the 3d metal and 2p oxygen band centers provides a covalent bond between the reactants and the electrocatalyst.[218,219] Additionally, by removing an oxygen atom from the transition metal oxide lattice, the two electrons that previously occupied the 2p oxygen orbitals tend to delocalize around the metal cation addictive to the oxygen vacancy.[217] This effect causes a decrease in the required overpotential and therefore facilitates certain electrochemical processes such as the oxidation of HMF.[107,200]

When there are oxygen vacancies in metal oxides, the electronic configuration of transition metal cations is affected, facilitating a high spin configuration in such a way that it can easily form bonds with OH^-. In this way, the formation of the M–OH intermediate is promoted and the ion transfer between the metal cation and the adsorbed reaction intermediates is improved.[217] By studying the OER, it has been determined that a high-spin electronic configuration promotes the electrophilicity of the adsorbed M–O and, therefore, the reaction between M–O and OH^- to form the intermediate M–OOH, which is usually a determining step in the rate of this reaction.[220] These effects contribute to lowering the kinetic energy barriers of multielement steps and speed up reaction kinetics.[221] Particularly, oxygen vacancies in cobalt-based transition metal oxide

Table 6 Electrocatalytic performance of different electrode materials using metal oxides and spinel oxides on the electrooxidation of HMF towards FDCA

System	[HMF]	Electrolyte	E_{onset}, V *vs.* RHE	FDCA yield	FE	Ref.
MnO_x	20 mM	1 M H_2SO_4	1.6	53.8%	33.8%	91
δ-MnO_2/NF	10 mM	1 M KOH	1.35	98%	98%	159
TiO_x@MnO_x	100 mM	0.1 M $HClO_4$	1.44	24%	—	209
NiO-CMK-1	20 mM	0.1 M KOH	1.85	—	70%	211
$NiCo_2O_4$ nanowires/NF	10 mM	0.1 M KOH	1.55	90%	∼100%	160
$NiCo_2O_4$/NF	5 mM	1 M KOH	1.5	—	87.5%	161
$CuCo_2O_4$/NF	50 mM	1 M KOH	1.23	93.7%	94%	162

electrocatalysts have been extensively studied due to the improvements they have presented against reactions such as OER, HER[222–225] and electrochemical oxidation of HMF.[107,200]

Z. Xiao *et al.* (2020) constructed pristine spinel oxide (Co_3O_4) and rich in oxygen vacancies (V_O) as electrocatalysts in order to study the mechanism of defects and their dynamic behavior towards OER electrocatalysis.[225] It was determined that V_O could facilitate the pre-oxidation of low valent Co (Co^{2+}) at a relatively lower applied potential. From this observation it was confirmed that V_O could initialize the reconstruction of the V_O–Co_3O_4 surface before the OER process occurs. Furthermore, it was shown that the oxygen vacancies were filled with OH^* first for V_O–Co_3O_4 facilitating the pre-oxidation of Co^{2+} and promoting the reconstruction/deprotonation of the Co–OOH^* intermediate. Therefore, the OER performance depends on the oxygen vacancies, which is directly related to the relative ratio of surface Co^{2+}/Co^{3+}.[226,227]

X. Huang *et al.* (2020) found that the electrocatalytic performance of cobalt oxide (CoO) could be significantly improved by introducing oxygen vacancies through Se doping for the electrochemical production of FDCA from HMF.[200] The CoO–$CoSe_2$ obtained with a CoO/$CoSe_2$ molar ratio of 23 : 1 presented a high yield of 99% and great stability for the production of FDCA with a faradaic efficiency of 97.9% at a potential of 1.43 V (*vs.* RHE). Furthermore, it was indicated that the introduction of V_O given by the selenization of CoO led to a high electrochemical active surface area and a low charge transfer resistance, improving the catalytic activity for the electrooxidation of HMF to FDCA.

Recently, R. Zhong *et al.* (2022) reported ultrathin polycrystalline Co_3O_4 nanosheets with enriched oxygen vacancies (Co_3O_4–V_O) synthesized by rapid calcination of the solvothermally synthesized ultrathin cobalt oxide hydrate (CoO_xH_y) nanosheets for electrochemical OER and electro oxidation of HMF to FDCA.[107] The Co_3O_4–V_O nanosheets exhibited higher electrocatalytic activity than the as-synthesized CoO_xH_y nanosheets and the conventionally calcined Co_3O_4 nanosheets in OER and especially in HMF electrooxidation. Co_3O_4–V_O required an overpotential of 312 mV to drive a current density of 10 mA cm^{-2} in HMF electrooxidation, while the as-synthesized CoO_xH_y and the conventionally calcined Co_3O_4 required overpotentials of 338 mV and 340 mV respectively. In this work it was indicated that richer V_O at the smaller Co_3O_4 nanograin boundaries of Co_3O_4–V_O can lead to the higher electrochemical surface area and low charge transfer resistance, therefore better electrocatalytic activity for HMF oxidation. Under the potential of 1.52 V (*vs.* RHE), 61% yield and 56% faradaic efficiency of FDCA were obtained with Co_3O_4–V_O.

In a recent work, M. Sun *et al.* (2022) also worked with Co(II) and Co(III) spinel oxide. In order to mediate the electrochemical oxidation of HMF, he developed a controllable nitrogen doping strategy to significantly improve the catalytic activity of Co_3O_4 nanowires on nickel foam (N–Co_3O_4/NF).[163] It was reported that N dopants can induce the formation of oxygen vacancies and together modulate the electronic structure of Co element and improve the conductivity of Co_3O_4 to the formation of electrocatalytically active sites. As a result, the electro-oxidation potential for HMF was 1.38 V (*vs.* RHE) when the current density reached 50 mA cm^{-2}. The conversion rate of HMF was 99.5%, and the yield of FDCA achieved 96.4%.

Table 7 presents the electrocatalytic performance of different electrode materials using oxygen vacancies.

In general terms, a wide variety of materials have been used as bifunctional electrodes for the production of H_2 and FDCA. According to the information presented in this section, it can be noted that the use of NFs has been notably highlighted due to its performance against both reactions. Its three-dimensional porous material gives it a large electroactive area as well as improved electrical conductivity, allowing it to be a suitable modification substrate and at the same time can reduce energy cost at both the cathode and anode. Regarding the use of noble metals, although they are known to be excellent electrocatalysts against other reactions such as HER and OER, they are not as effective in reducing the required overpotential or in increasing the efficiency of FDCA electroproduction. By contrast, the transition metals are notably cheaper than the noble metals and also present several possibilities of electronic configurations of the 3d orbitals, giving them structural versatility in the generation of bi- or trimetallic alloys towards the simultaneous

Table 7 Electrocatalytic performance of different electrode materials using oxygen vacancies on the electrooxidation of HMF towards FDCA

System	[HMF]	Electrolyte	E_{onset}, V *vs.* RHE	FDCA yield	FE	Ref.
Co_3O_4–V_O	5 mM	1 M KOH	1.52	61%	56%	107
CoO–$CoSe_2$	10 mM	0.1 M KOH	1.43	99%	97.9%	200
N–Co_3O_4/NF	50 mM	1 M KOH	1.38	96.4%	99.5%	163

production of H_2 and FDCA. In the case of mixed transition metals, it can be seen that when they are used as electrocatalysts they present prominent results. Particularly, when Ni is incorporated into the structure of the mixed transition metals, low onset potential values, high HMF conversion rates and excellent selectivity are achieved towards FDCA production that is reflected in high yields and faradaic efficiencies. Some bi- and trimetallic oxides and spinel oxides present interesting interactions between their components that allow the introduction of oxygen vacancies to promote better adsorption of reagents and intermediates, and to modulate the exposure of active sites. It can be observed that those mixed metal oxides as well as spinel oxides that contain Co in their structure improve the performance in the electrooxidation of HMF to FDCA, especially if these structures are applied on NFs.

5. Conversion and distribution in the production OF H_2 and FDCA

The simultaneous electrochemical production of H_2 and FDCA can be carried out experimentally in an H-type electrolysis cell (with two compartments) such as the one illustrated in Fig. 6. This cell corresponds to a completely sealed device in such a way that there is no exchange of gases between the interior and the exterior, and between both half-cells, which are also separated by a salt bridge. Both simultaneous electrochemical reactions are usually carried out in alkaline electrolyte, in such a way that the product of the HMF electrooxidation reaction is liquid FDCA (it was already discussed above that an acidic electrolyte leads to the formation of solid FDCA). The alkaline electrolyte must be previously saturated with an inert gas (*e.g.* Ar).

A constant potential is applied, whose value will be determined by the energy requirement of the material used in the anode and cathode so that both reactions can occur. The study of the potential to be applied is previously carried out through linear or cyclic voltammetry. Once conversion begins to generate products, gaseous H_2 is produced in the cathode half-cell and liquid FDCA (in alkaline electrolyte) in the anode half-cell. While the electrocatalysis is carried out, the electrolyte solution is kept under magnetic agitation, favoring the ascent of the hydrogen bubbles towards the upper space of the half-cell called headspace.

The production of H_2 gas is usually monitored by Gas Chromatography (GC),[228] while the conversion of HMF and the distribution of possible products, in addition to FDCA, are analyzed by High Performance Liquid Chromatography (HPLC).[107]

By way of example, hydrogen and oxygen generated by water electrolysis have been detected by L. Liao *et al.* (2013), who took samples with a syringe (Gastight) and measured them using a SP-6890 Gas Chromatograph equipped with a thermal conduction detector (Gow-Mac).[229] In addition, a mass spectrometer (SRS residual gas analyzer, RGA200) was obtained to identify the isotopic gas species from the water splitting. Gaseous H_2 obtained from water splitting has also been detected and quantified by H. Lei *et al.* (2014) by gas chromatography during electrolysis at 1.0 V (*vs.* Ag/AgCl) under anaerobic conditions and at room temperature.[228] T. E. Rosser *et al.* (2016) also detected and quantified the amount of H_2 produced during the photocatalytic water electrolysis.[230] In H_2 quantification, the cell was purged with N_2/CH_4 (2%) for 10 min before electrochemical experiments. The $0H_2$ produced was quantified using an Agilent 7890A gas chromatograph, with CH_4 as internal standard.

On the other hand, B. You *et al.* (2016) analyzed HMF oxidation products by taking 10 μL of the electrolyte solution during chronoamperometry at 1.423 V *vs.* RHE (for three-electrode configuration) of the electrolyte solution and diluted with 490 μL with water and then studied by HPLC on a Shimadzu Prominence LC-2030C system at room temperature.[54] The HPLC was equipped with an ultraviolet-visible detector set at 265 nm and a 4.6 mm × 150 mm Shim-pack GWS 5 μm C 18 column. A mixture of elution solvents corresponding to 70% aqueous 5 mM ammonium formate solution and 30% methanol was used, for a 10 min run time and a flow rate of 0.5 mL min^{-1}. The identification and quantification of the products were determined from the calibration curves by applying standard solutions with known concentrations of commercially purchased pure reagents, intermediate products, and final products.

The conversion of HMF (%) and yields (%) of the oxidation products are usually calculated as the following:[107]

$$\text{HMF conversion } (\%) = \frac{\text{mol of HMF consumed}}{\text{mol of initial HMF}} \times 100\%$$

$$\text{Product yield } (\%) = \frac{\text{mol of product formed}}{\text{mol of initial HMF}} \times 100\%$$

The faradaic efficiency (FE) of FDCA is calculated using the following equations where F represents Faraday's constant, 96 485 C mol^{-1}:

$$\text{FE}_{\text{FDCA}} \ (\%) = \frac{\text{mol of FDCA formed}}{\text{charge passed}/(F \times 6)} \times 100\%$$

In those cases where the selectivity towards the production of FDCA is less than 100%, the faradaic efficiency of the intermediate products possibly formed (DFF, HFCA and FFCA) can be studied as follows:

$$\text{FE}_{\text{DFF}} \ (\%) = \frac{\text{mol of DFF formed}}{\text{charge passed}/(F \times 2)} \times 100\%$$

$$\text{FE}_{\text{HMFCA}} \ (\%) = \frac{\text{mol of HMFCA formed}}{\text{charge passed}/(F \times 2)} \times 100\%$$

$$\text{FE}_{\text{FFCA}} \ (\%) = \frac{\text{mol of FFCA formed}}{\text{charge passed}/(F \times 4)} \times 100\%$$

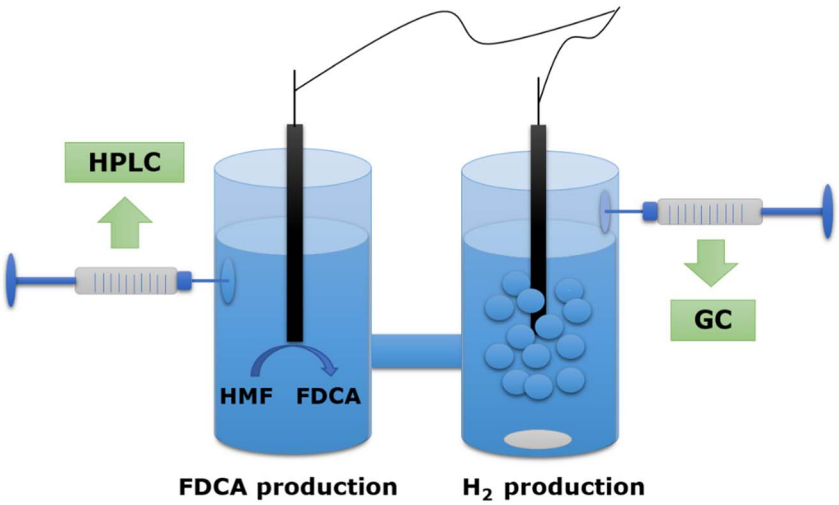

Fig. 6 Representation of an H-type electrolysis cell suitable for the simultaneous electrochemical production of liquid FDCA and gaseous H_2. Both products can be followed by HPLC and GC respectively.

6. Upcoming challenges

One of the main challenges is the design of both H_2 and FDCA production systems, in economically and environmentally appropriate scenarios for both their generation and their application. Given the renewable and abundant nature of the compounds derived from biomass, the biorefinery plays a fundamental role in achieving a transition towards the production of chemical products and fuels in replacement of the current and predominant industry based on fossil sources.

The electrocatalytic conversion of biomass-derived compounds, particularly the leading platform candidates, to value-added products (*e.g.* biofuels, value-added chemicals, green solvents, *etc.*) represents an attractive and novel strategy for the production on a large scale. Although novel electrocatalytic systems have been reported for the biorefining of biomass platform molecules such as HMF, their short-term commercialization is still limited by the lack of understanding of their electrocatalytic mechanisms, which result in less control of product selectivity (FDCA). In this regard, new theoretical investigations should be able to provide more detailed information about the electrocatalytic pathways in various types of active sites.

In a complementary way, considering the coupled production of H_2 and FDCA, it is assumed adequate to have infrastructure to provide electrical energy obtained from renewable sources, in such a way that both products can be classified as "green". Moreover, since the electrooxidation of biomass platform molecules (such as HMF) is usually carried out at high pH values, it is urgent to improve the efficiency and stability of the electrodes against H_2 production under alkaline conditions. In this way it will be more feasible to use simultaneous production methods in coupled systems. Additionally, more efforts are required to improve the storage and transport systems for the H_2 produced.

The following challenges must largely focus on the design and synthesis of new materials to be used as electrodes against electrochemical reactions to produce H_2 and FDCA. These materials must meet a series of requirements that include mechanical, chemical and electrochemical stability to ensure a long useful life. In addition, they must present good electrocatalytic characteristics towards both reactions in such a way as to reduce the energy requirements for production in terms of onset potential, present high faradaic efficiencies, show a robust and reproducible electrochemical response. The electrocatalysts, when functioning as anodes, must show selectivity towards obtaining FDCA, avoiding the formation of intermediate reaction products. These materials must be cheap, able to be obtained from abundant sources on the planet and be friendly to the environment. In this sense, it is of great importance to continue testing new combinations of materials that enhance their mechanical and physicochemical properties to allow bifunctional materials to be obtained that meet the aforementioned requirements. In this way it will be possible to guarantee the simultaneous production of H_2 and FDCA efficiently and successfully.

The first study related to the electrochemical conversion of HMF to FDCA emerged 3 decades ago, however it took a long time before this topic generated interest in the scientific community. In fact, the largest number of electrocatalysts have been reported in the second half of the last decade. Meanwhile, the electrochemical production of H_2 has not ceased to be studied. Thus, the current challenge is to continue working on the manufacture of electrodes capable of functioning as efficient electrocatalysts for both reactions.

Although noble metal-based electrodes are highly electrocatalytic and efficient towards HER, they have been shown to be unsuitable for carrying out HMF electrooxidation, presenting higher overpotentials, low conversion percentages and undesirable efficiencies. Therefore, it is necessary to continue the search for new alternatives, such as those related to non-noble metals.

Some transition metals have been extensively studied towards the coupled electrochemical production of H_2 and FDCA, and in addition to being considerably more abundant and cheaper than the noble metals, they show outstanding activity and efficiency in both reactions. Mixed non-noble transition metal electrocatalysts with Ni content have presented outstanding results, showing low

onset potential values, high HMF conversion rates with excellent selectivity towards FDCA production that is reflected in an increase in yield and faradaic efficiency. For this reason, it is interesting to continue understanding the electrocatalytic mechanisms to develop new alternatives that enhance the chemical properties of Ni.

Due to its amazing electrocatalytic properties, it is also of great importance to innovate in the use of new metal non-oxides and metal oxides. Some bi- and trimetallic oxides and spinel oxides present interesting interactions between their components that give them novel opportunities for their applicability. Therefore, more efforts are required to understand in detail its structural and electronic architecture and its reaction mechanisms associated with the electrochemical oxidation of HMF and HER. In this way, it will be easier to continue innovating in the introduction of oxygen vacancies to promote better adsorption of reagents and intermediates, increase conductivity, decrease resistance to charge transfer, and even modulate the electroactive area through greater exposure of electroactive sites.

In addition, in order to be economically competitive, the search for electrocatalyst materials must continue, not only composed of elements with the greatest abundance on the planet, but it is also relevant that they have been synthesized through economic and eco-friendly methods.

Due to the high volatility of power generation and the dynamically related interdependencies within a factory system, a valid technical, economic and environmental assessment of the benefits induced by H_2 technologies can currently only be achieved using digital factory models.[49] It is also necessary to improve the quality of the electrochemical production methods of H_2 and FDCA in large volumes to be scaled at an industrial and commercial level, optimizing the reaction media, and minimizing the energy costs of the production of FDCA (according to the materials of the electrocatalysts used). In order to guarantee both the circular economy and the decarbonization of the industry, it is interesting to study and evaluate the use of H_2 as a fuel to generate energy and/or heat on an industrial scale and use it, for example, in the same factories where bioplastics (PEF) are produced from FDCA.

Within this context, it is also desirable to improve the large-scale production of PEF (and related materials, such as food and beverage packaging) to make the selective production of FDCA by electrochemical means more viable and attractive. On the other hand, the raw materials used for the synthesis of FDCA have a great impact on the production cost of FDCA. For this reason, the use of lignocellulosic waste as potential low-cost substrates should be further exploited for the development of such processes. Therefore, to achieve the success of large-scale H_2 and FDCA production, all the required technical, economic and environmental challenges must be taken into account.

7. Conclusions

In summary, this work addressed the simultaneous electrocatalytic production of H_2 from water and FDCA from HMF, with the aim of advancing towards the production of clean electrical energy and at the same time making sustainable use of forest biomass that is currently accumulated as waste. Likewise, the benefits of carrying out the simultaneous electrochemical production of H_2 and FDCA compared to traditional water electrolysis with H_2 and O_2 production were presented. In this sense, the energetic suitability of the HMF electrocatalysis coupling was highlighted given its favored thermodynamics that reduce the potential required by the overall reaction, replacing the production of O_2. The importance of producing FDCA as a product with higher added value compared to the O_2 generated in the traditional electrochemical separation of water was also recognized, as well as obtaining an aqueous anodic product, avoiding the undesired formation of the H_2/O_2 gas mixture.

Through an exploration of the materials recently used as bifunctional electrocatalysts for the production of H_2 and FDCA, the wide use of NF was highlighted for being a three-dimensional porous material with a large electroactive area and excellent electrical conductivity, which allows not only to act as modification substrate but is also able to reduce the energy cost of both reactions. Through the studies reported in recent years, it is possible to note that, although noble metals are exceptional electrocatalysts for the production of H_2, they fail to reduce the required overpotentials or increase the efficiency in obtaining FDCA. On the other hand, the non-noble transition metals are considerably cheaper and due to their varied possibilities of electronic configurations of the 3d orbitals, they are highly versatile for generating attractive and efficient bimetallic or trimetallic alloys towards the co-production of H_2 and FDCA. Some non-noble transition metal mixed electrocatalysts have presented outstanding results, especially when Ni has been incorporated into their structure, showing low onset potential values, high HMF conversion rates with excellent selectivity towards FDCA production that is reflected in high yields and faradaic efficiencies. In addition, the reported spinel oxides show interactions between their components that present attractive opportunities in the introduction of oxygen vacancies to promote better adsorption of reactants and intermediates, improve conductivity, decrease resistance to charge transfer, and modulate the exposure of the active sites through an increase in the electroactive surface.

Finally, it is stated that future projections and challenges in the simultaneous electrochemical production of H_2 and FDCA should focus on detailed understanding of the architecture and electronic structure of materials and electrocatalytic mechanisms to ensure higher conductivities, greater exposure of the electroactive sites, better adsorption of reagents and intermediates, and faster reaction kinetics. On the other hand, work must continue in the search for economically convenient materials, abundant on the planet and synthesized with environmentally friendly methods. To ensure the simultaneous production of H_2 and FDCA on a large scale and its prompt implementation in the industrial world, it is essential to work on upcoming technical, economic and environmental evaluations. It is also necessary to improve the quality of the electrochemical production methods of H_2 and FDCA in large volumes to be scaled up commercially, guaranteeing the circular economy, the decarbonisation of industrial processes and a sustainable use of renewable resources.

Abbreviations

HMF	5-Hydroxymethylfurfural
DES	Deep eutectic solvent
DFF	Diformyl furan
Eonset	Onset potential
FDCA	2,5-Furandicarboxylic acid
FE	Faradaic efficiency
FFCA	5-Formyl-furoic acid
GC	Gas chromatography
H_2	Molecular hydrogen
HER	Hydrogen evolution reaction
HMFCA	5-Hydroxymethyl-2 furan carboxylic acid
HOR	Hydrogen oxidation reaction
HPLC	High-performance liquid chromatography
MOF	Metal–organic framework
NF	Nickel foam
OER	Oxygen evolution reaction
ORR	Oxygen reduction reaction
PEF	Polyethylene furanoate
PEM	Proton exchange membrane
PET	Polyethylene terephthalate
SMR	Steam methane reforming
TPA	Terephthalic acid
V_O	Oxygen vacancies

Conflicts of interest

The authors declare no conflict or competing financial interest.

Acknowledgements

The author, LG is grateful to the ANID Postdoctoral scholarship 2022 #3220040. JA acknowledges ANID, Fondecyt Regular No. 1230561 and Proyecto 20CEIN2-142146 Consorcio Sur-Sub-antártico CI2030. GR acknowledges ANID, Fondecyt Regular No. 1220107.

References

1 B. M. Opeyemi, Path to sustainable energy consumption: the possibility of substituting renewable energy for non-renewable energy, *Energy*, 2021, **228**, 120519, DOI: 10.1016/j.energy.2021.120519.
2 D. Shindell and C. J. Smith, Climate and air-quality benefits of a realistic phase-out of fossil fuels, *Nature*, 2019, **573**, 408–411, DOI: 10.1038/s41586-019-1554-z.
3 X. Xu, Z. Wei, Q. Ji, C. Wang and G. Gao, Global renewable energy development: influencing factors, trend predictions and countermeasures, *Resour. Policy*, 2019, **63**, 101470, DOI: 10.1016/j.resourpol.2019.101470.
4 Z. Zhongming, L. Linong, Y. Xiaona, Z. Wangqiang and L. Wei, *IPCC meetings go carbon-neutral*, 2018, https://119.78.100.173/C666/handle/2XK7JSWQ/219911.
5 D. Bogdanov, M. Ram, A. Aghahosseini, A. Gulagi, A. S. Oyewo, M. Child, *et al.*, Low-cost renewable electricity as the key driver of the global energy transition towards sustainability, *Energy*, 2021, **227**, 120467, DOI: 10.1016/j.energy.2021.120467.
6 T. T. Delbole and D. Ajayi, From Waste to Energy; Comparative Assessment of Heat Values of Biomass Briquettes and Fuel Wood for Bio-fuel Utilization and Strategic Waste Management in Ethiopia, *Int. J. Innovative Sci. Res. Technol.*, 2021, **6**(4), 896–903.
7 F. L. Braghiroli and L. Passarini, Valorization of biomass residues from forest operations and wood manufacturing presents a wide range of sustainable and innovative possibilities, *Current Forestry Reports*, 2020, **6**, 172–183, DOI: 10.1007/s40725-020-00112-9.
8 Renewable Energy Market - Analysis, Size & Report - Industry Overview, (s.f.), Home | Mordor Intelligence, https://www.mordorintelligence.com/industry-reports/global-renewable-energy-market-industry.
9 Renewable Energy Market Size, Share Analysis | Growth Forecast - 2030, (s.f.), *Allied Market Research*, https://www.alliedmarketresearch.com/renewable-energy-market.
10 P. Amoatey, A. Al-Hinai, A. Al-Mamun and M. S. Baawain, A review of recent renewable energy status and potentials in Oman, *Sustainable Energy Technologies and Assessments*, 2022, **51**, 101919, DOI: 10.1016/j.seta.2021.101919.
11 M. Y. Worku, Recent Advances in Energy Storage Systems for Renewable Source Grid Integration: A Comprehensive Review, *Sustainability*, 2022, **14**, 5985, DOI: 10.3390/su14105985.
12 J.-Y. Lee, S.-E. Lee and D.-W. Lee, Current status and future prospects of biological routes to bio-based products using raw materials, wastes, and residues as renewable resources, *Crit. Rev. Environ. Sci. Technol.*, 2022, **52**, 2453–2509, DOI: 10.1080/10643389.2021.1880259.
13 S. Jabeen, A comparative systematic literature review and bibliometric analysis on sustainability of renewable energy sources, *Int. J. Energ. Econ. Pol.*, 2020, **11**(1), 270–280, DOI: 10.32479/ijeep.10759.
14 D. Maradin, Advantages and disadvantages of renewable energy sources utilization, *Int. J. Energy Econ. Policy*, 2021, **11**(3), 176–183, DOI: 10.32479/ijeep.11027.
15 A. Suyarov, U. Sorimsokov, B. Narimanov and M. Nasullayev, Use of solar and wind energy sources in autonomous networks, *Web of Scientist: International Scientific Research Journal*, 2022, **3**, 219–225, DOI: 10.17605/OSF.IO/HVSZ5.
16 J. B. Goodenough, Electrochemical energy storage in a sustainable modern society, *Energy Environ. Sci.*, 2014, **7**, 14–18, DOI: 10.1039/C3EE42613K.
17 J. Liu, J. G. Zhang, Z. Yang, J. P. Lemmon, C. Imhoff, G. L. Graff, *et al.*, Materials science and materials chemistry for large scale electrochemical energy storage: from transportation to electrical grid, *Adv. Funct. Mater.*, 2013, **23**, 929–946, DOI: 10.1002/adfm.201200690.
18 H. D. Yoo, E. Markevich, G. Salitra, D. Sharon and D. Aurbach, On the challenge of developing advanced technologies for electrochemical energy storage and

conversion, *Mater. Today*, 2014, **17**, 110–121, DOI: 10.1016/j.mattod.2014.02.014.

19 A. R. Razmi, S. M. Alirahmi, M. H. Nabat, E. Assareh and M. Shahbakhti, A green hydrogen energy storage concept based on parabolic trough collector and proton exchange membrane electrolyzer/fuel cell: thermodynamic and exergoeconomic analyses with multi-objective optimization, *Int. J. Hydrogen Energy*, 2022, **47**(64), 26468–26489, DOI: 10.1016/j.ijhydene.2022.03.021.

20 A. Olabi, A. A. Abdelghafar, A. Baroutaji, E. T. Sayed, A. H. Alami, H. Rezk, *et al.*, Large-vscale hydrogen production and storage technologies: current status and future directions, *Int. J. Hydrogen Energy*, 2021, **46**, 23498–23528, DOI: 10.1016/j.ijhydene.2020.10.110.

21 E. Tosun and M. Özcanlı, Hydrogen enrichment effects on performance and emission characteristics of a diesel engine operated with diesel-soybean biodiesel blends with nanoparticle addition, *Eng. Sci. Technol.*, 2021, **24**, 648–654, DOI: 10.1016/j.jestch.2020.12.022.

22 R. Singh, M. Singh and S. Gautam, Hydrogen economy, energy, and liquid organic carriers for its mobility, *Mater. Today: Proc.*, 2021, **46**, 5420–5427, DOI: 10.1016/j.matpr.2020.09.065.

23 M. Hermesmann and T. Müller, Green, Turquoise, Blue, Or Grey? Environmentally Friendly Hydrogen Production in Transforming Energy Systems, *Prog. Energy Combust. Sci.*, 2022, **90**, 100996, DOI: 10.1016/j.pecs.2022.100996.

24 S. F. Ahmed, M. Mofijur, S. Nuzhat, N. Rafa, A. Musharrat, S. S. Lam, *et al.*, Sustainable hydrogen production: technological advancements and economic analysis, *Int. J. Hydrogen Energy*, 2022, **47**, 37227–37255, DOI: 10.1016/j.ijhydene.2021.12.029.

25 M. Yu, K. Wang and H. Vredenburg, Insights into low-carbon hydrogen production methods: green, blue and aqua hydrogen, *Int. J. Hydrogen Energy*, 2021, **46**, 21261–21273, DOI: 10.1016/j.ijhydene.2021.04.016.

26 N. Z. Muradov and T. N. Veziroğlu, "Green" path from fossil-based to hydrogen economy: an overview of carbon-neutral technologies, *Int. J. Hydrogen Energy*, 2008, **33**, 6804–6839, DOI: 10.1016/j.ijhydene.2008.08.054.

27 L. Mosca, J. A. M. Jimenez, S. A. Wassie, F. Gallucci, E. Palo, M. Colozzi, *et al.*, Process design for green hydrogen production, *Int. J. Hydrogen Energy*, 2020, **45**, 7266–7277, DOI: 10.1016/j.ijhydene.2019.08.206.

28 M. Ostadi, K. G. Paso, S. Rodriguez-Fabia, L. E. Øi, F. Manenti and M. Hillestad, Process integration of green hydrogen: decarbonization of chemical industries, *Energies*, 2020, **13**, 4859, DOI: 10.3390/en13184859.

29 M. Newborough and G. Cooley, Green hydrogen: the only oxygen and water balanced fuel, *Fuel Cell. Bull.*, 2021, 16–19, DOI: 10.1016/S1464-2859(21)00169-3.

30 H. Xiang, P. Ch, M. A. Nawaz, S. Chupradit, A. Fatima and M. Sadiq, Integration and economic viability of fueling the future with green hydrogen: an integration of its determinants from renewable economics, *Int. J. Hydrogen Energy*, 2021, **46**, 38145–38162, DOI: 10.1016/j.ijhydene.2021.09.067.

31 D. Jang, J. Kim, D. Kim, W.-B. Han and S. Kang, Techno-economic analysis and Monte Carlo simulation of green hydrogen production technology through various water electrolysis technologies, *Energy Convers. Manage.*, 2022, **258**, 115499, DOI: 10.1016/j.enconman.2022.115499.

32 Hydrogen-based Renewable Energy Market, (s.f.), Market Research Reports, Business Consulting | In-depth Insights | TMR, https://www.transparencymarketresearch.com/hydrogen-based-renewable-energy-market.html.

33 Green Hydrogen Market Analysis & Future Trends Report, (s.f.), MarketsandMarkets, https://www.marketsandmarkets.com/Market-Reports/green-hydrogen-market-92444177.html.

34 K. Jiao, J. Xuan, Q. Du, Z. Bao, B. Xie, B. Wang, *et al.*, Designing the next generation of proton-exchange membrane fuel cells, *Nature*, 2021, **595**, 361–369, DOI: 10.1038/s41586-021-03482-7.

35 F. Xiao, Y. C. Wang, Z. P. Wu, G. Chen, F. Yang, S. Zhu, *et al.*, Recent advances in electrocatalysts for proton exchange membrane fuel cells and alkaline membrane fuel cells, *Adv. Mater.*, 2021, **33**, 2006292, DOI: 10.1002/adma.202006292.

36 Y. Wang, D. F. R. Diaz, K. S. Chen, Z. Wang and X. C. Adroher, Materials, technological status, and fundamentals of PEM fuel cells–a review, *Mater. Today*, 2020, **32**, 178–203, DOI: 10.1016/j.mattod.2019.06.005.

37 Y. Manoharan, S. E. Hosseini, B. Butler, H. Alzhahrani, B. T. F. Senior, T. Ashuri, *et al.*, Hydrogen fuel cell vehicles; current status and future prospect, *Appl. Sci.*, 2019, **9**, 2296, DOI: 10.3390/app9112296.

38 H. Choi, J. Shin and J. Woo, Effect of electricity generation mix on battery electric vehicle adoption and its environmental impact, *Energy Policy*, 2018, **121**, 13–24, DOI: 10.1016/j.enpol.2018.06.013.

39 G. J. Offer, D. Howey, M. Contestabile, R. Clague and N. Brandon, Comparative analysis of battery electric, hydrogen fuel cell and hybrid vehicles in a future sustainable road transport system, *Energy Policy*, 2010, **38**, 24–29, DOI: 10.1016/j.enpol.2009.08.040.

40 M. G. Sürer and H. T. Arat, Advancements and current technologies on hydrogen fuel cell applications for marine vehicles, *Int. J. Hydrogen Energy*, 2022, **47**, 19865–19875, DOI: 10.1016/j.ijhydene.2021.12.251.

41 O. B. Inal and C. Deniz, Assessment of fuel cell types for ships: based on multi-criteria decision analysis, *J. Cleaner Prod.*, 2020, **265**, 121734, DOI: 10.1016/j.jclepro.2020.121734.

42 M. G. Sürer and H. T. Arat, State of Art of Hydrogen Usage as a Fuel on Aviation, *Eur. Mech. Sci.*, 2018, **2**, 20–30, DOI: 10.26701/ems.364286.

43 K. Şenel, *Hidrojenin yakıt olarak uçaklarda kullanımı ESOGÜ*, Fen Bilimleri Enstitüsü, 2007.

44 J. M. Krawczyk, A. M. Mazur, T. Sasin and A. Stokłosa, Fuel cells as alternative power for unmanned aircraft systems–current situation and development trends, *Pr. Inst. Lotnictwa*, 2014, **4**, 49–62.

45 G. D. Brewer, *Hydrogen aircraft technology*, Routledge, 2017, DOI: 10.1201/9780203751480.
46 D. Cecere, E. Giacomazzi and A. Ingenito, A review on hydrogen industrial aerospace applications, *Int. J. Hydrogen Energy*, 2014, **39**, 10731–10747, DOI: 10.1016/j.ijhydene.2014.04.126.
47 A. Baroutaji, T. Wilberforce, M. Ramadan and A. G. Olabi, Comprehensive investigation on hydrogen and fuel cell technology in the aviation and aerospace sectors, *Renewable Sustainable Energy Rev.*, 2019, **106**, 31–40, DOI: 10.1016/j.rser.2019.02.022.
48 Z. Pu, G. Zhang, A. Hassanpour, D. Zheng, S. Wang, S. Liao, *et al.*, Regenerative fuel cells: recent progress, challenges, perspectives and their applications for space energy system, *Applied Energy*, 2021, **283**, 116376, DOI: 10.1016/j.apenergy.2020.116376.
49 C. Imdahl, C. Blume, S. Blume, S. Zellmer, M. Gensicke and C. Herrmann, Potentials of hydrogen technologies for sustainable factory systems, *Procedia CIRP*, 2021, **98**, 583–588, DOI: 10.1016/j.procir.2021.01.1580.
50 O. Oner and K. Khalilpour, Evaluation of green hydrogen carriers: a multi-criteria decision analysis tool, *Renewable Sustainable Energy Rev.*, 2022, **168**, 112764, DOI: 10.1016/j.rser.2022.112764.
51 A. Eftekhari, Electrocatalysts for hydrogen evolution reaction, *Int. J. Hydrogen Energy*, 2017, **42**, 11053–11077, DOI: 10.1016/j.ijhydene.2017.02.125.
52 B. You, N. Jiang, X. Liu and Y. Sun, Simultaneous H_2 Generation and Biomass Upgrading in Water by an Efficient Noble-Metal-Free Bifunctional Electrocatalyst, *Angew. Chem., Int. Ed.*, 2016, **55**, 9913–9917, DOI: 10.1002/anie.201603798.
53 M. M. Ibrahim, F. A. Agblevor and W. K. El-Zawawy, Isolation and characterization of cellulose and lignin from steam-exploded lignocellulosic biomass, *BioResources*, 2010, **5**, 397–418.
54 B. You, X. Liu, N. Jiang and Y. Sun, A general strategy for decoupled hydrogen production from water splitting by integrating oxidative biomass valorization, *J. Am. Chem. Soc.*, 2016, **138**, 13639–13646, DOI: 10.1021/jacs.6b07127.
55 M. Sajid, X. Zhao and D. Liu, Production of 2,5-furandicarboxylic acid (FDCA) from 5-hydroxymethylfurfural (HMF): recent progress focusing on the chemical-catalytic routes, *Green Chem.*, 2018, **20**, 5427–5453, DOI: 10.1039/C8GC02680G.
56 S. Zhang, G. Shen, Y. Deng, Y. Lei, J.-W. Xue, Z. Chen, *et al.*, Efficient synthesis of 2,5-furandicarboxylic acid from furfural based platform through aqueous-phase carbonylation, *ACS Sustain. Chem. Eng.*, 2018, **6**, 13192–13198, DOI: 10.1021/acssuschemeng.8b02780.
57 J. Wang, X. Liu, J. Zhu and Y. Jiang, Copolyesters based on 2,5-furandicarboxylic acid (FDCA): effect of 2,2,4,4-tetramethyl-1,3-cyclobutanediol units on their properties, *Polymers*, 2017, **9**, 305, DOI: 10.3390/polym9090305.
58 A. F. Sousa, C. Vilela, A. C. Fonseca, M. Matos, C. S. Freire, G.-J. M. Gruter, *et al.*, Biobased polyesters and other polymers from 2,5-furandicarboxylic acid: a tribute to furan excellency, *Polym. Chem.*, 2015, **6**, 5961–5983, DOI: 10.1039/C5PY00686D.
59 G. Z. Papageorgiou, D. G. Papageorgiou, Z. Terzopoulou and D. N. Bikiaris, Production of bio-based 2,5-furan dicarboxylate polyesters: recent progress and critical aspects in their synthesis and thermal properties, *Eur. Polym. J.*, 2016, **83**, 202–229, DOI: 10.1016/j.eurpolymj.2016.08.004.
60 K.-R. Hwang, W. Jeon, S. Y. Lee, M.-S. Kim and Y.-K. Park, Sustainable bioplastics: recent progress in the production of bio-building blocks for the bio-based next-generation polymer PEF, *Chem. Eng. J.*, 2020, **390**, 124636, DOI: 10.1016/j.cej.2020.124636.
61 Y. Kwon, K. J. P. Schouten, J. C. van der Waal, E. de Jong and M. T. Koper, Electrocatalytic conversion of furanic compounds, *ACS Catal.*, 2016, **6**, 6704–6717, DOI: 10.1021/acscatal.6b01861.
62 S. Pandey, M.-J. Dumont, V. Orsat and D. Rodrigue, Biobased 2,5-furandicarboxylic acid (FDCA) and its emerging copolyesters' properties for packaging applications, *Eur. Polym. J.*, 2021, **160**, 110778, DOI: 10.1016/j.eurpolymj.2021.110778.
63 T. R. Boussie, E. L. Dias, Z. M. Fresco and V. J. Murphy, Production of adipic acid and derivatives from carbohydrate-containing materials, *US Pat.*, 8,501,989, US8501989B2, 6 Aug. 2013.
64 T. Werpy and G. Petersen, *Top value added chemicals from biomass: volume I–results of screening for potential candidates from sugars and synthesis gas*, National Renewable Energy Lab, Golden, CO, USA, 2004, DOI: 10.2172/15008859.
65 S. K. Burgess, J. E. Leisen, B. E. Kraftschik, C. R. Mubarak, R. M. Kriegel and W. J. Koros, Chain mobility, thermal, and mechanical properties of poly(ethylene furanoate) compared to poly(ethylene terephthalate), *Macromolecules*, 2014, **47**, 1383–1391, DOI: 10.1021/ma5000199.
66 S. K. Burgess, O. Karvan, J. Johnson, R. M. Kriegel and W. J. Koros, Oxygen sorption and transport in amorphous poly(ethylene furanoate), *Polymer*, 2014, **55**, 4748–4756, DOI: 10.1016/j.polymer.2014.07.041.
67 A. Eerhart, A. Faaij and M. Patel, Replacing fossil based PET with biobased PEF; process analysis, energy and GHG balance, *Energy Environ. Sci.*, 2012, **5**, 6407–6422, DOI: 10.1039/C2EE02480B.
68 J. Cai, K. Li and S. Wu, Recent advances in catalytic conversion of biomass derived 5-hydroxymethylfurfural into 2,5-furandicarboxylic acid, *Biomass Bioenergy*, 2022, **158**, 106358, DOI: 10.1016/j.biombioe.2022.106358.
69 E. de Jong, H. A. Visser, A. S. Dias, C. Harvey and G.-J. M. Gruter, The Road to Bring FDCA and PEF to the Market, *Polymers*, 2022, **14**, 943, DOI: 10.3390/polym14050943.
70 F. R. Duke and T. W. Haas, The homogeneous base-catalyzed decomposition of hydrogen peroxide1, *J. Phys. Chem.*, 1961, **65**, 304–306, DOI: 10.1021/j100820a028.
71 R. O. Rajesh, T. K. Godan, R. Sindhu, A. Pandey and P. Binod, Bioengineering advancements, innovations and

challenges on green synthesis of 2,5-furan dicarboxylic acid, *Bioengineered*, 2020, **11**, 19–38, DOI: 10.1080/21655979.2019.1700093.

72 T. S. Hansen, I. Sádaba, E. J. García-Suárez and A. Riisager, Cu catalyzed oxidation of 5-hydroxymethylfurfural to 2,5-diformylfuran and 2,5-furandicarboxylic acid under benign reaction conditions, *Appl. Catal., A*, 2013, **456**, 44–50, DOI: 10.1016/j.apcata.2013.01.042.

73 B. Saha, S. Dutta and M. M. Abu-Omar, Aerobic oxidation of 5-hydroxylmethylfurfural with homogeneous and nanoparticulate catalysts, *Catal. Sci. Technol.*, 2012, **2**, 79–81, DOI: 10.1039/C1CY00321F.

74 Z. Zhang and K. Deng, Recent advances in the catalytic synthesis of 2,5-furandicarboxylic acid and its derivatives, *ACS Catal.*, 2015, **5**, 6529–6544, DOI: 10.1021/acscatal.5b01491.

75 G. Yi, S. P. Teong and Y. Zhang, The Direct Conversion of Sugars into 2,5-Furandicarboxylic Acid in a Triphasic System, *ChemSusChem*, 2015, **8**, 1151–1155, DOI: 10.1002/cssc.201500118.

76 L. Dessbesell, S. Souzanchi, K. T. Venkateswara Rao, A. A. Carrillo, D. Bekker, K. A. Hall, *et al.*, Production of 2,5-furandicarboxylic acid (FDCA) from starch, glucose, or high-fructose corn syrup: techno-economic analysis, *Biofuels, Bioprod. Biorefin.*, 2019, **13**, 1234–1245, DOI: 10.1002/bbb.2014.

77 G. Yi, S. P. Teong, X. Li and Y. Zhang, Purification of Biomass-Derived 5-Hydroxymethylfurfural and Its Catalytic Conversion to 2,5-Furandicarboxylic Acid, *ChemSusChem*, 2014, **7**, 2131–2135, DOI: 10.1002/cssc.201402105.

78 M. L. Ribeiro and U. Schuchardt, Cooperative effect of cobalt acetylacetonate and silica in the catalytic cyclization and oxidation of fructose to 2,5-furandicarboxylic acid, *Catal. Commun.*, 2003, **4**, 83–86, DOI: 10.1016/S1566-7367(02)00261-3.

79 M. Kröger, U. Prüße and K.-D. Vorlop, A new approach for the production of 2,5-furandicarboxylic acid by in situ oxidation of 5-hydroxymethylfurfural starting from fructose, *Top. Catal.*, 2000, **13**, 237–242, DOI: 10.1023/A:1009017929727.

80 R. Wojcieszak and I. Itabaiana, Engineering the future: perspectives in the 2,5-furandicarboxylic acid synthesis, *Catal. Today*, 2020, **354**, 211–217, DOI: 10.1016/j.cattod.2019.05.071.

81 A. H. Motagamwala, W. Won, C. Sener, D. M. Alonso, C. T. Maravelias and J. A. Dumesic, Toward biomass-derived renewable plastics: production of 2,5-furandicarboxylic acid from fructose, *Sci. Adv.*, 2018, **4**, eaap9722, DOI: 10.1126/sciadv.aap9722.

82 A. H. Motagamwala, K. Huang, C. T. Maravelias and J. A. Dumesic, Solvent system for effective near-term production of hydroxymethylfurfural (HMF) with potential for long-term process improvement, *Energy Environ. Sci.*, 2019, **12**, 2212–2222, DOI: 10.1039/C9EE00447E.

83 K. Iris, D. C. Tsang, A. C. Yip, A. J. Hunt, J. Sherwood, J. Shang, *et al.*, Propylene carbonate and γ-valerolactone as green solvents enhance Sn(IV)-catalysed hydroxymethylfurfural (HMF) production from bread waste, *Green Chem.*, 2018, **20**, 2064–2074, DOI: 10.1039/C8GC00358K.

84 Y. Li, X. Wei, L. Chen and J. Shi, Electrocatalytic hydrogen production trilogy, *Angew. Chem., Int. Ed.*, 2021, **60**, 19550–19571, DOI: 10.1002/anie.202009854.

85 C. Chen, L. Wang, B. Zhu, Z. Zhou, S. I. El-Hout, J. Yang, *et al.*, 2,5-Furandicarboxylic acid production via catalytic oxidation of 5-hydroxymethylfurfural: catalysts, processes and reaction mechanism, *J. Energy Chem.*, 2021, **54**, 528–554, DOI: 10.1016/j.jechem.2020.05.068.

86 Y. Meng, S. Yang and H. Li, Electro-and Photocatalytic Oxidative Upgrading of Bio-based 5-Hydroxymethylfurfural, *ChemSusChem*, 2022, **15**, e202102581, DOI: 10.1002/cssc.202102581.

87 W. Partenheimer and V. V. Grushin, Synthesis of 2,5-Diformylfuran and Furan-2,5-Dicarboxylic Acid by Catalytic Air-Oxidation of 5-Hydroxymethylfurfural. Unexpectedly Selective Aerobic Oxidation of Benzyl Alcohol to Benzaldehyde with Metal = Bromide Catalysts, *Adv. Synth. Catal.*, 2001, **343**, 102–111, DOI: 10.1002/1615-4169(20010129)343:1<102::AID-ADSC102>3.0.CO;2-Q.

88 P. Verdeguer, N. Merat and A. Gaset, Oxydation catalytique du HMF en acide 2,5-furane dicarboxylique, *J. Mol. Catal.*, 1993, **85**, 327–344, DOI: 10.1016/0304-5102(93)80059-4.

89 Y. Yang and T. Mu, Electrochemical oxidation of biomass derived 5-hydroxymethylfurfural (HMF): pathway, mechanism, catalysts and coupling reactions, *Green Chem.*, 2021, **23**, 4228–4254, DOI: 10.1039/D1GC00914A.

90 Y. Zhao, M. Cai, J. Xian, Y. Sun and G. Li, Recent advances in the electrocatalytic synthesis of 2,5-furandicarboxylic acid from 5-(hydroxymethyl)furfural, *J. Mater. Chem. A*, 2021, **9**, 20164–20183, DOI: 10.1039/D1TA04981J.

91 S. R. Kubota and K. S. Choi, Electrochemical Oxidation of 5-Hydroxymethylfurfural to 2,5-Furandicarboxylic Acid (FDCA) in Acidic Media Enabling Spontaneous FDCA Separation, *ChemSusChem*, 2018, **11**, 2138–2145, DOI: 10.1002/cssc.201800532.

92 S. C. Lai, S. E. Kleijn, F. T. Öztürk, V. C. van Rees Vellinga, J. Koning, P. Rodriguez, *et al.*, Effects of electrolyte pH and composition on the ethanol electro-oxidation reaction, *Catal. Today*, 2010, **154**, 92–104, DOI: 10.1016/j.cattod.2010.01.060.

93 M. T. Koper, Theory of multiple proton–electron transfer reactions and its implications for electrocatalysis, *Chem. Sci.*, 2013, **4**, 2710–2723, DOI: 10.1039/C3SC50205H.

94 J. Joo, T. Uchida, A. Cuesta, M. T. Koper and M. Osawa, Importance of acid–base equilibrium in electrocatalytic oxidation of formic acid on platinum, *J. Am. Chem. Soc.*, 2013, **135**, 9991–9994, DOI: 10.1021/ja403578s.

95 Y. Kwon, S. C. Lai, P. Rodriguez and M. T. Koper, Electrocatalytic oxidation of alcohols on gold in alkaline media: base or gold catalysis?, *J. Am. Chem. Soc.*, 2011, **133**, 6914–6917, DOI: 10.1021/ja200976j.

96 B. N. Zope, D. D. Hibbitts, M. Neurock and R. J. Davis, Reactivity of the gold/water interface during selective

oxidation catalysis, *Science*, 2010, **330**, 74–78, DOI: 10.1126/science.1195055.

97 W. C. Ketchie, M. Murayama and R. J. Davis, Promotional effect of hydroxyl on the aqueous phase oxidation of carbon monoxide and glycerol over supported Au catalysts, *Top. Catal.*, 2007, **44**, 307–317, DOI: 10.1007/s11244-007-0304-x.

98 M. Coronas, Y. Holade and D. Cornu, Review of the Electrospinning Process and the Electro-Conversion of 5-Hydroxymethylfurfural (HMF) into Added-Value Chemicals, *Materials*, 2022, **15**, 4336, DOI: 10.3390/ma15124336.

99 J. Zhang, W. Gong, H. Yin, D. Wang, Y. Zhang, H. Zhang, *et al.*, In situ growth of ultrathin $Ni(OH)_2$ nanosheets as catalyst for electrocatalytic oxidation reactions, *ChemSusChem*, 2021, **14**, 2935–2942, DOI: 10.1002/cssc.202100811.

100 R. Zhang, S. Jiang, Y. Rao, S. Chen, Q. Yue and Y. Kang, Electrochemical biomass upgrading on CoOOH nanosheets in a hybrid water electrolyzer, *Green Chem.*, 2021, **23**, 2525–2530, DOI: 10.1039/D0GC04157B.

101 P. Zhang, X. Sheng, X. Chen, Z. Fang, J. Jiang, M. Wang, *et al.*, Paired electrocatalytic oxygenation and hydrogenation of organic substrates with water as the oxygen and hydrogen source, *Angew. Chem.*, 2019, **131**, 9253–9257, DOI: 10.1002/ange.201903936.

102 Z. Zhou, Y.-n. Xie, L. Sun, Z. Wang, W. Wang, L. Jiang, *et al.*, Strain-induced in situ formation of NiOOH species on CoCo bond for selective electrooxidation of 5-hydroxymethylfurfural and efficient hydrogen production, *Appl. Catal., B*, 2022, **305**, 121072, DOI: 10.1016/j.apcatb.2022.121072.

103 Y. Zhong, R.-Q. Ren, L. Qin, J.-B. Wang, Y.-Y. Peng, Q. Li, *et al.*, Electrodeposition of hybrid nanosheet-structured $NiCo_2O_4$ on carbon fiber paper as a non-noble electrocatalyst for efficient electrooxidation of 5-hydroxymethylfurfural to 2,5-furandicarboxylic acid, *New J. Chem.*, 2021, **45**, 11213–11221, DOI: 10.1039/D1NJ01489G.

104 G. Yang, Y. Jiao, H. Yan, Y. Xie, A. Wu, X. Dong, *et al.*, Interfacial engineering of MoO_2-FeP heterojunction for highly efficient hydrogen evolution coupled with biomass electrooxidation, *Adv. Mater.*, 2020, **32**, 2000455, DOI: 10.1002/adma.202000455.

105 W.-J. Liu, L. Dang, Z. Xu, H.-Q. Yu, S. Jin and G. W. Huber, Electrochemical oxidation of 5-hydroxymethylfurfural with NiFe layered double hydroxide (LDH) nanosheet catalysts, *ACS Catal.*, 2018, **8**, 5533–5541, DOI: 10.1021/acscatal.8b01017.

106 B. Zhang, H. Fu and T. Mu, Hierarchical NiS_x/Ni_2P nanotube arrays with abundant interfaces for efficient electrocatalytic oxidation of 5-hydroxymethylfurfural, *Green Chem.*, 2022, **24**, 877–884, DOI: 10.1039/D1GC04206H.

107 R. Zhong, Q. Wang, L. Du, Y. Pu, S. Ye, M. Gu, *et al.*, Ultrathin polycrystalline Co_3O_4 nanosheets with enriched oxygen vacancies for efficient electrochemical oxygen evolution and 5-hydroxymethylfurfural oxidation, *Appl. Surf. Sci.*, 2022, **584**, 152553, DOI: 10.1016/j.apsusc.2022.152553.

108 F. Suleman, I. Dincer and M. Agelin-Chaab, Environmental impact assessment and comparison of some hydrogen production options, *Int. J. Hydrogen Energy*, 2015, **40**, 6976–6987, DOI: 10.1016/j.ijhydene.2015.03.123.

109 M. Luo, Y. Yi, S. Wang, Z. Wang, M. Du, J. Pan, *et al.*, Review of hydrogen production using chemical-looping technology, *Renewable Sustainable Energy Rev.*, 2018, **81**, 3186–3214, DOI: 10.1016/j.rser.2017.07.007.

110 M. Younas, S. Shafique, A. Hafeez, F. Javed and F. Rehman, An overview of hydrogen production: current status, potential, and challenges, *Fuel*, 2022, **316**, 123317, DOI: 10.1016/j.fuel.2022.123317.

111 M. N. Uddin, W. W. Daud and H. F. Abbas, Potential hydrogen and non-condensable gases production from biomass pyrolysis: insights into the process variables, *Renewable Sustainable Energy Rev.*, 2013, **27**, 204–224, DOI: 10.1016/j.rser.2013.06.031.

112 X. Hu and M. Gholizadeh, Biomass pyrolysis: a review of the process development and challenges from initial researches up to the commercialisation stage, *J. Energy Chem.*, 2019, **39**, 109–143, DOI: 10.1016/j.jechem.2019.01.024.

113 M. Taherdanak, H. Zilouei and K. Karimi, Investigating the effects of iron and nickel nanoparticles on dark hydrogen fermentation from starch using central composite design, *Int. J. Hydrogen Energy*, 2015, **40**, 12956–12963, DOI: 10.1016/j.ijhydene.2015.08.004.

114 M. M. Tezcan, A. G. Yetgin, A. I. Canakoglu, B. Cevher, M. Turan, M. Ayaz, *et al.*, *MATEC Web of Conferences*, EDP Sciences, 2018.

115 N. H. M. Yasin, T. Mumtaz, M. A. Hassan and N. A. Rahman, Food waste and food processing waste for biohydrogen production: a review, *J. Environ. Manage.*, 2013, **130**, 375–385, DOI: 10.1016/j.jenvman.2013.09.009.

116 T. Jarunglumlert, C. Prommuak, N. Putmai and P. Pavasant, Scaling-up bio-hydrogen production from food waste: feasibilities and challenges, *Int. J. Hydrogen Energy*, 2018, **43**, 634–648, DOI: 10.1016/j.ijhydene.2017.10.013.

117 Z. Wei, J. Liu and W. Shangguan, A review on photocatalysis in antibiotic wastewater: pollutant degradation and hydrogen production, *Chin. J. Catal.*, 2020, **41**, 1440–1450, DOI: 10.1016/S1872-2067(19)63448-0.

118 R. Kothari, D. Buddhi and R. Sawhney, Comparison of environmental and economic aspects of various hydrogen production methods, *Renewable Sustainable Energy Rev.*, 2008, **12**, 553–563, DOI: 10.1016/j.rser.2006.07.012.

119 J. Chi and H. Yu, Water electrolysis based on renewable energy for hydrogen production, *Chin. J. Catal.*, 2018, **39**, 390–394, DOI: 10.1016/S1872-2067(17)62949-8.

120 P. Nikolaidis and A. Poullikkas, A comparative overview of hydrogen production processes, *Renewable Sustainable Energy Rev.*, 2017, **67**, 597–611, DOI: 10.1016/j.rser.2016.09.044.

121 F. Rehman, W. S. Abdul Majeed and W. B. Zimmerman, Hydrogen production from water vapor plasmolysis using DBD-Corona hybrid reactor, *Energy Fuels*, 2013, **27**, 2748–2761, DOI: 10.1021/ef301981f.

122 I. Pushkareva, A. Pushkarev, S. Grigoriev, P. Modisha and D. Bessarabov, Comparative study of anion exchange membranes for low-cost water electrolysis, *Int. J. Hydrogen Energy*, 2020, **45**, 26070–26079, DOI: 10.1016/j.ijhydene.2019.11.011.

123 B. Rausch, M. D. Symes, G. Chisholm and L. Cronin, Decoupled catalytic hydrogen evolution from a molecular metal oxide redox mediator in water splitting, *Science*, 2014, **345**, 1326–1330, DOI: 10.1126/science.1257443.

124 X. Liu, R. Guo, K. Ni, F. Xia, C. Niu, B. Wen, *et al.*, Reconstruction-determined alkaline water electrolysis at industrial temperatures, *Adv. Mater.*, 2020, **32**, 2001136, DOI: 10.1002/adma.202001136.

125 G. H. C. Reduction, *Scaling up electrolysers to meet the 1.5 C climate goal*, International Renewable Energy Agency, Abu Dhabi, 2020.

126 D. Li, E. J. Park, W. Zhu, Q. Shi, Y. Zhou, H. Tian, *et al.*, Highly quaternized polystyrene ionomers for high performance anion exchange membrane water electrolysers, *Nat. Energy*, 2020, **5**, 378–385, DOI: 10.1038/s41560-020-0577-x.

127 T. Wang, Z. Huang, T. Liu, L. Tao, J. Tian, K. Gu, *et al.*, Transforming electrocatalytic biomass upgrading and hydrogen production from electricity input to electricity output, *Angew. Chem.*, 2022, **134**, e202115636, DOI: 10.1002/ange.202115636.

128 P. Muthukumar, D. Moon and S. P. Anthony, Copper coordination polymer electrocatalyst for strong hydrogen evolution reaction activity in neutral medium: influence of coordination environment and network structure, *Catal. Sci. Technol.*, 2019, **9**, 4347–4354, DOI: 10.1039/C9CY00759H.

129 Y. Zhang, X. Xia, X. Cao, B. Zhang, N. H. Tiep, H. He, *et al.*, Ultrafine metal nanoparticles/N-doped porous carbon hybrids coated on carbon fibers as flexible and binder-free water splitting catalysts, *Adv. Energy Mater.*, 2017, **7**, 1700220, DOI: 10.1002/aenm.201700220.

130 W. Zhou, J. Jia, J. Lu, L. Yang, D. Hou, G. Li, *et al.*, Recent developments of carbon-based electrocatalysts for hydrogen evolution reaction, *Nano Energy*, 2016, **28**, 29–43, DOI: 10.1016/j.nanoen.2016.08.027.

131 S. Ramakrishna, D. S. Reddy, S. S. Kumar and V. Himabindu, Nitrogen doped CNTs supported palladium electrocatalyst for hydrogen evolution reaction in PEM water electrolyser, *Int. J. Hydrogen Energy*, 2016, **41**, 20447–20454, DOI: 10.1016/j.ijhydene.2016.08.195.

132 S. Shiva Kumar, S. Ramakrishna, B. Rama Devi and V. Himabindu, Phosphorus-doped graphene supported palladium (Pd/PG) electrocatalyst for the hydrogen evolution reaction in PEM water electrolysis, *Int. J. Green Energy*, 2018, **15**, 558–567, DOI: 10.1080/15435075.2018.1508468.

133 S. Shiva Kumar, S. Ramakrishna, B. Rama Devi and V. Himabindu, Phosphorus-doped carbon nanoparticles supported palladium electrocatalyst for the hydrogen evolution reaction (HER) in PEM water electrolysis, *Ionics*, 2018, **24**, 3113–3121, DOI: 10.1007/s11581-018-2471-0.

134 S. Shiva Kumar and V. Himabindu, Hydrogen production by PEM water electrolysis–a review, *Mater. Sci. Energy Technol.*, 2019, **2**, 442–454, DOI: 10.1016/j.mset.2019.03.002.

135 B. B. Beyene, S. B. Mane and C.-H. Hung, Electrochemical hydrogen evolution by cobalt(II) porphyrins: effects of ligand modification on catalytic activity, efficiency and overpotential, *J. Electrochem. Soc.*, 2018, **165**, H481, DOI: 10.1149/2.0481809jes.

136 S. Cui, M. Qian, X. Liu, Z. Sun and P. Du, A Copper Porphyrin-Based Conjugated Mesoporous Polymer-Derived Bifunctional Electrocatalyst for Hydrogen and Oxygen Evolution, *ChemSusChem*, 2016, **9**, 2365–2373, DOI: 10.1002/cssc.201600452.

137 M. Natali, A. Luisa, E. Iengo and F. Scandola, Efficient photocatalytic hydrogen generation from water by a cationic cobalt(II) porphyrin, *Chem. Commun.*, 2014, **50**, 1842–1844, DOI: 10.1039/C3CC48882A.

138 G. Grabowski, J. Lewkowski and R. Skowroński, The electrochemical oxidation of 5-hydroxymethylfurfural with the nickel oxide/hydroxide electrode, *Electrochim. Acta*, 1991, **36**, 1995, DOI: 10.1016/0013-4686(91)85084-K.

139 K. Li and Y. Sun, Electrocatalytic upgrading of biomass-derived intermediate compounds to value-added products, *Chem.–Eur. J.*, 2018, **24**, 18258–18270, DOI: 10.1002/chem.201803319.

140 N. Jiang, B. You, R. Boonstra, I. M. Terrero Rodriguez and Y. Sun, Integrating electrocatalytic 5-hydroxymethylfurfural oxidation and hydrogen production via Co–P-derived electrocatalysts, *ACS Energy Lett.*, 2016, **1**, 386–390, DOI: 10.1021/acsenergylett.6b00214.

141 V. H. Nguyen and J.-J. Shim, In situ growth of hierarchical mesoporous $NiCo_2S_4$@MnO_2 arrays on nickel foam for high-performance supercapacitors, *Electrochim. Acta*, 2015, **166**, 302–309, DOI: 10.1016/j.electacta.2015.03.069.

142 F. García-Moreno, Commercial applications of metal foams: their properties and production, *Materials*, 2016, **9**, 85, DOI: 10.3390/ma9020085.

143 S. Peng, L. Li, H. B. Wu, S. Madhavi and X. W. Lou, Controlled growth of $NiMoO_4$ nanosheet and nanorod arrays on various conductive substrates as advanced electrodes for asymmetric supercapacitors, *Adv. Energy Mater.*, 2015, **5**, 1401172, DOI: 10.1002/aenm.201401172.

144 A. Muzaffar, M. B. Ahamed, K. Deshmukh and J. Thirumalai, A review on recent advances in hybrid supercapacitors: design, fabrication and applications, *Renewable Sustainable Energy Rev.*, 2019, **101**, 123–145, DOI: 10.1016/j.rser.2018.10.026.

145 Q. He, S. Gu, T. Wu, S. Zhang, X. Ao, J. Yang, *et al.*, Self-supported mesoporous $FeCo_2O_4$ nanosheets as high

capacity anode material for sodium-ion battery, *Chem. Eng. J.*, 2017, **330**, 764–773, DOI: 10.1016/j.cej.2017.08.014.

146 R. M. Obodo, N. M. Shinde, U. K. Chime, S. Ezugwu, A. C. Nwanya, I. Ahmad, *et al.*, Recent advances in metal oxide/hydroxide on three-dimensional nickel foam substrate for high performance pseudocapacitive electrodes, *Curr. Opin. Electrochem.*, 2020, **21**, 242–249, DOI: 10.1016/j.coelec.2020.02.022.

147 S. H. Ahn, S. J. Hwang, S. J. Yoo, I. Choi, H.-J. Kim, J. H. Jang, *et al.*, Electrodeposited Ni dendrites with high activity and durability for hydrogen evolution reaction in alkaline water electrolysis, *J. Mater. Chem.*, 2012, **22**, 15153–15159, DOI: 10.1039/C2JM31439H.

148 Y. Xiao, Y. Liu, Z. Tang, L. Wu, Y. Zeng, Y. Xu, *et al.*, Porous Ni–Cr–Fe alloys as cathode materials for the hydrogen evolution reaction, *RSC Adv.*, 2016, **6**, 51096–51105, DOI: 10.1039/C6RA07316F.

149 I. Herraiz-Cardona, E. Ortega, L. Vázquez-Gómez and V. Pérez-Herranz, Double-template fabrication of three-dimensional porous nickel electrodes for hydrogen evolution reaction, *Int. J. Hydrogen Energy*, 2012, **37**, 2147–2156, DOI: 10.1016/j.ijhydene.2011.09.155.

150 K. Siwek, S. Eugénio, D. Santos, M. Silva and M. Montemor, 3D nickel foams with controlled morphologies for hydrogen evolution reaction in highly alkaline media, *Int. J. Hydrogen Energy*, 2019, **44**, 1701–1709, DOI: 10.1016/j.ijhydene.2018.11.070.

151 D. M. Santos, C. A. Sequeira and J. L. Figueiredo, Hydrogen production by alkaline water electrolysis, *Quim. Nova*, 2013, **36**, 1176–1193, DOI: 10.1590/S0100-40422013000800017.

152 R. Latsuzbaia, R. Bisselink, A. Anastasopol, H. Van der Meer, R. Van Heck, M. S. Yagüe, *et al.*, Continuous electrochemical oxidation of biomass derived 5-(hydroxymethyl)furfural into 2,5-furandicarboxylic acid, *J. Appl. Electrochem.*, 2018, **48**, 611–626, DOI: 10.1007/s10800-018-1157-7.

153 A. Delparish, A. Uslu, Y. Cao, T. de Groot, J. van der Schaaf, T. Noël, *et al.*, Boosting the valorization of biomass and green electrons to chemical building blocks: a study on the kinetics and mass transfer during the electrochemical conversion of HMF to FDCA in a microreactor, *Chem. Eng. J.*, 2022, **438**, 135393, DOI: 10.1016/j.cej.2022.135393.

154 M. Fleischmann, K. Korinek and D. Pletcher, The oxidation of hydrazine at a nickel anode in alkaline solution, *J. Electroanal. Chem. Interfacial Electrochem.*, 1972, **34**, 499–503, DOI: 10.1016/S0022-0728(72)80425-X.

155 W. Visscher and E. Barendrecht, Investigation of thin-film α-and β-$Ni(OH)_2$ electrodes in alkaline solutions, *J. Electroanal. Chem. Interfacial Electrochem.*, 1983, **154**, 69–80, DOI: 10.1016/S0022-0728(83)80532-4.

156 W. Chen, C. Xie, Y. Wang, Y. Zou, C.-L. Dong, Y.-C. Huang, *et al.*, Activity origins and design principles of nickel-based catalysts for nucleophile electrooxidation, *Chem*, 2020, **6**, 2974–2993, DOI: 10.1016/j.chempr.2020.07.022.

157 Y. Zhong, R.-Q. Ren, J.-B. Wang, Y.-Y. Peng, Q. Li and Y.-M. Fan, Grass-like Ni_xSe_y nanowire arrays shelled with NiFe LDH nanosheets as a 3D hierarchical core–shell electrocatalyst for efficient upgrading of biomass-derived 5-hydroxymethylfurfural and furfural, *Catal. Sci. Technol.*, 2022, **12**, 201–211, DOI: 10.1039/D1CY01816G.

158 S. Barwe, J. Weidner, S. Cychy, D. M. Morales, S. Dieckhöfer, D. Hiltrop, *et al.*, Electrocatalytic oxidation of 5-(hydroxymethyl)furfural using high-surface-area nickel boride, *Angew. Chem., Int. Ed.*, 2018, **57**, 11460–11464, DOI: 10.1002/anie.201806298.

159 C. Wang, H.-J. Bongard, C. Weidenthaler, Y. Wu and F. Schüth, Design and Application of a High-Surface-Area Mesoporous δ-MnO_2 Electrocatalyst for Biomass Oxidative Valorization, *Chem. Mater.*, 2022, **34**, 3123–3132, DOI: 10.1021/acs.chemmater.1c04223.

160 L. Gao, Y. Bao, S. Gan, Z. Sun, Z. Song, D. Han, *et al.*, Hierarchical nickel–cobalt-based transition metal oxide catalysts for the electrochemical conversion of biomass into valuable chemicals, *ChemSusChem*, 2018, **11**, 2547–2553, DOI: 10.1002/cssc.201800695.

161 M. J. Kang, H. Park, J. Jegal, S. Y. Hwang, Y. S. Kang and H. G. Cha, Electrocatalysis of 5-hydroxymethylfurfural at cobalt based spinel catalysts with filamentous nanoarchitecture in alkaline media, *Appl. Catal., B*, 2019, **242**, 85–91, DOI: 10.1016/j.apcatb.2018.09.087.

162 Y. Lu, C. L. Dong, Y. C. Huang, Y. Zou, Z. Liu, Y. Liu, *et al.*, Identifying the geometric site dependence of spinel oxides for the electrooxidation of 5-hydroxymethylfurfural, *Angew. Chem., Int. Ed.*, 2020, **59**, 19215–19221, DOI: 10.1002/anie.202007767.

163 M. Sun, Y. Wang, C. Sun, Y. Qi, J. Cheng, Y. Song, *et al.*, Nitrogen-doped Co_3O_4 nanowires enable high-efficiency electrochemical oxidation of 5-hydroxymethylfurfural, *Chin. Chem. Lett.*, 2022, **33**, 385–389, DOI: 10.1016/j.cclet.2021.05.009.

164 K. R. Vuyyuru and P. Strasser, Oxidation of biomass derived 5-hydroxymethylfurfural using heterogeneous and electrochemical catalysis, *Catal. Today*, 2012, **195**, 144–154, DOI: 10.1016/j.cattod.2012.05.008.

165 D. J. Chadderdon, L. Xin, J. Qi, Y. Qiu, P. Krishna, K. L. More, *et al.*, Electrocatalytic oxidation of 5-hydroxymethylfurfural to 2,5-furandicarboxylic acid on supported Au and Pd bimetallic nanoparticles, *Green Chem.*, 2014, **16**, 3778–3786, DOI: 10.1039/C4GC00401A.

166 M. Park, M. Gu and B.-S. Kim, Tailorable electrocatalytic 5-hydroxymethylfurfural oxidation and H_2 production: architecture–performance relationship in bifunctional multilayer electrodes, *ACS Nano*, 2022, **14**, 6812–6822, DOI: 10.1021/acsnano.0c00581.

167 T. Cao, M. Wu, V. V. Ordomsky, X. Xin, H. Wang, P. Métivier, *et al.*, Selective electrogenerative oxidation of 5-hydroxymethylfurfural to 2,5-furandialdehyde, *ChemSusChem*, 2017, **10**, 4851–4854, DOI: 10.1002/cssc.201702119.

168 G.-R. Xu, M. Batmunkh, S. Donne, H. Jin, J.-X. Jiang, Y. Chen, *et al.*, Ruthenium(III) polyethyleneimine complexes for bifunctional ammonia production and biomass upgrading, *J. Mater. Chem. A*, 2019, **7**, 25433–25440, DOI: 10.1039/C9TA10267A.

169 Y. Du, H. Sheng, D. Astruc and M. Zhu, Atomically precise noble metal nanoclusters as efficient catalysts: a bridge between structure and properties, *Chem. Rev.*, 2019, **120**, 526–622, DOI: 10.1021/acs.chemrev.8b00726.

170 M. A. Ayude, L. I. Doumic, M. C. Cassanello and K. D. Nigam, Clean catalytic oxidation for derivatization of key biobased platform chemicals: ethanol, glycerol, and hydroxymethyl furfural, *Ind. Eng. Chem. Res.*, 2019, **58**, 16077–16095, DOI: 10.1021/acs.iecr.9b00977.

171 M. Guo, X. Lu, J. Xiong, R. Zhang, X. Li, Y. Qiao, *et al.*, Alloy-Driven Efficient Electrocatalytic Oxidation of Biomass-Derived 5-Hydroxymethylfurfural towards 2,5-Furandicarboxylic Acid: A Review, *ChemSusChem*, 2022, **15**, e202201074, DOI: 10.1002/cssc.202201074.

172 C. Wei, S. Sun, D. Mandler, X. Wang, S. Z. Qiao and Z. J. Xu, Approaches for measuring the surface areas of metal oxide electrocatalysts for determining their intrinsic electrocatalytic activity, *Chem. Soc. Rev.*, 2019, **48**, 2518–2534, DOI: 10.1039/C8CS00848E.

173 P. Qi, S. Chen, J. Chen, J. Zheng, X. Zheng and Y. Yuan, Catalysis and reactivation of ordered mesoporous carbon-supported gold nanoparticles for the base-free oxidation of glucose to gluconic acid, *ACS Catal.*, 2015, **5**, 2659–2670, DOI: 10.1021/cs502093b.

174 R. Wojcieszak, C. P. Ferraz, J. Sha, S. Houda, L. M. Rossi and S. Paul, Advances in base-free oxidation of bio-based compounds on supported gold catalysts, *Catalysts*, 2017, **7**, 352, DOI: 10.3390/catal7110352.

175 A. Markusse, B. Kuster and J. Schouten, Platinum catalysed aqueous methyl α-d-glucopyranoside oxidation in a multiphase redox-cycle reactor, *Catal. Today*, 2001, **66**, 191–197, DOI: 10.1016/S0920-5861(00)00648-9.

176 M. A. Lilga, R. T. Hallen and M. Gray, Production of oxidized derivatives of 5-hydroxymethylfurfural (HMF), *Top. Catal.*, 2010, **53**, 1264–1269, DOI: 10.1007/s11244-010-9579-4.

177 X. Zhong, Y. Wei, S. Sadjadi, D. Liu, M. Li, T. Yu, *et al.*, Base-free oxidation of 5-hydroxymethylfurfural to 2,5-furandicarboxylic acid over palygorskite-supported bimetallic Pt–Pd catalyst, *Appl. Clay Sci.*, 2022, **226**, 106574, DOI: 10.1016/j.clay.2022.106574.

178 H. G. Cha and K.-S. Choi, Combined biomass valorization and hydrogen production in a photoelectrochemical cell, *Nat. Chem.*, 2015, **7**, 328–333, DOI: 10.1038/nchem.2194.

179 C. Zhou, W. Shi, X. Wan, Y. Meng, Y. Yao, Z. Guo, *et al.*, Oxidation of 5-hydroxymethylfurfural over a magnetic iron oxide decorated rGO supporting Pt nanocatalyst, *Catal. Today*, 2019, **330**, 92–100, DOI: 10.1016/j.cattod.2018.05.037.

180 A. R. Poerwoprajitno, L. Gloag, J. Watt, S. Cychy, S. Cheong, P. V. Kumar, *et al.*, Faceted branched nickel nanoparticles with tunable branch length for high-activity electrocatalytic oxidation of biomass, *Angew. Chem., Int. Ed.*, 2020, **59**, 15487–15491, DOI: 10.1002/anie.202005489.

181 T. Gao, Y. Yin, G. Zhu, Q. Cao and W. Fang, Co_3O_4 NPs decorated Mn-Co-O solid solution as highly selective catalyst for aerobic base-free oxidation of 5-HMF to 2,5-FDCA in water, *Catal. Today*, 2020, **355**, 252–262, DOI: 10.1016/j.cattod.2019.03.065.

182 J. N. Hausmann, R. Beltrán-Suito, S. Mebs, V. Hlukhyy, T. F. Fässler, H. Dau, *et al.*, Evolving Highly Active Oxidic Iron(III) Phase from Corrosion of Intermetallic Iron Silicide to Master Efficient Electrocatalytic Water Oxidation and Selective Oxygenation of 5-Hydroxymethylfurfural, *Adv. Mater.*, 2021, **33**, 2008823, DOI: 10.1002/adma.202008823; C. Wang, H.-J. Bongard, C. Weidenthaler, Y. Wu and F. Schüth, Design and Application of a High-Surface-Area Mesoporous δ-MnO_2 Electrocatalyst for Biomass Oxidative Valorization, *Chem. Mater.*, 2022, **34**, 3123–3132, DOI: 10.1021/acs.chemmater.1c04223.

183 X. Pang, H. Bai, H. Zhao, W. Fan and W. Shi, Efficient electrocatalytic oxidation of 5-hydroxymethylfurfural coupled with 4-nitrophenol hydrogenation in a water system, *ACS Catal.*, 2022, **12**, 1545–1557, DOI: 10.1021/acscatal.1c04880.

184 F. Kong and M. Wang, Preparation of sulfur-modulated nickel/carbon composites from lignosulfonate for the electrocatalytic oxidation of 5-hydroxymethylfurfural to 2,5-furandicarboxylic acid, *ACS Appl. Energy Mater.*, 2021, **4**, 1182–1188, DOI: 10.1021/acsaem.0c02418.

185 S. Furukawa and T. Komatsu, Intermetallic compounds: promising inorganic materials for well-structured and electronically modified reaction environments for efficient catalysis, *ACS Catal.*, 2017, **7**, 735–765, DOI: 10.1021/acscatal.6b02603.

186 L. Rößner and M. Armbrüster, Electrochemical energy conversion on intermetallic compounds: a review, *ACS Catal.*, 2019, **9**, 2018–2062, DOI: 10.1021/acscatal.8b04566.

187 M. Cai, Y. Zhang, Y. Zhao, Q. Liu, Y. Li and G. Li, Two-dimensional metal–organic framework nanosheets for highly efficient electrocatalytic biomass 5-(hydroxymethyl) furfural (HMF) valorization, *J. Mater. Chem. A*, 2020, **8**, 20386–20392, DOI: 10.1039/D0TA07793C.

188 X. Deng, X. Kang, M. Li, K. Xiang, C. Wang, Z. Guo, *et al.*, Coupling efficient biomass upgrading with H_2 production via bifunctional Cu_xS@NiCo-LDH core–shell nanoarray electrocatalysts, *J. Mater. Chem. A*, 2020, **8**, 1138–1146, DOI: 10.1039/C9TA06917H.

189 C. Cheng, F. Zheng, C. Zhang, C. Du, Z. Fang, Z. Zhang, *et al.*, High-efficiency bifunctional electrocatalyst based on 3D freestanding Cu foam in situ armored CoNi alloy nanosheet arrays for overall water splitting, *J. Power Sources*, 2019, **427**, 184–193, DOI: 10.1016/j.jpowsour.2019.04.071.

190 Q. Zhang, X. L. Li, B. X. Tao, X. H. Wang, Y. H. Deng, X. Y. Gu, *et al.*, CoNi based alloy/oxides@N-doped carbon core-shell dendrites as complementary water splitting electrocatalysts with significantly enhanced catalytic efficiency, *Appl. Catal., B*, 2019, **254**, 634–646, DOI: 10.1016/j.apcatb.2019.05.035.

191 R. Zheng, C. Zhao, J. Xiong, X. Teng, W. Chen, Z. Hu, *et al.*, Construction of a hierarchically structured, NiCo–Cu-based trifunctional electrocatalyst for efficient overall water

splitting and 5-hydroxymethylfurfural oxidation, *Sustainable Energy Fuels*, 2021, **5**, 4023–4031, DOI: 10.1039/D1SE00697E.

192 M. Zhang, Y. Liu, B. Liu, Z. Chen, H. Xu and K. Yan, Trimetallic NiCoFe-layered double hydroxides nanosheets efficient for oxygen evolution and highly selective oxidation of biomass-derived 5-hydroxymethylfurfural, *ACS Catal.*, 2020, **10**, 5179–5189, DOI: 10.1021/acscatal.0c00007.

193 X.-J. Bai, W.-X. He, X.-Y. Lu, Y. Fu and W. Qi, Electrochemical oxidation of 5-hydroxymethylfurfural on ternary metal–organic framework nanoarrays: enhancement from electronic structure modulation, *J. Mater. Chem. A*, 2021, **9**, 14270–14275, DOI: 10.1039/D1TA02464G.

194 Z. Chen, Y. Song, J. Cai, X. Zheng, D. Han, Y. Wu, *et al.*, Tailoring the d-band centers enables Co_4N nanosheets to be highly active for hydrogen evolution catalysis, *Angew. Chem.*, 2018, **130**, 5170–5174, DOI: 10.1002/anie.201801834.

195 Q. Song, J. Li, S. Wang, J. Liu, X. Liu, L. Pang, *et al.*, Enhanced Electrocatalytic Performance through Body Enrichment of Co-Based Bimetallic Nanoparticles In Situ Embedded Porous N-Doped Carbon Spheres, *Small*, 2019, **15**, 1903395, DOI: 10.1002/smll.201903395.

196 G. Yang, Y. Jiao, H. Yan, C. Tian and H. Fu, Electronic Structure Modulation of Non-Noble-Metal-Based Catalysts for Biomass Electrooxidation Reactions, *Small Struct.*, 2021, **2**, 2100095, DOI: 10.1002/sstr.202100095.

197 S. Li, X. Sun, Z. Yao, X. Zhong, Y. Cao, Y. Liang, *et al.*, Biomass Valorization via Paired Electrosynthesis over Vanadium Nitride-Based Electrocatalysts, *Adv. Funct. Mater.*, 2019, **29**, 1904780, DOI: 10.1002/adfm.201904780.

198 M. Xing, D. Zhang, D. Liu, C. Song and D. Wang, Surface engineering of carbon-coated cobalt-doped nickel phosphides bifunctional electrocatalyst for boosting 5-hydroxymethylfurfural oxidation coupled with hydrogen evolution, *J. Colloid Interface Sci.*, 2023, **629**, 451–460, DOI: 10.1016/j.jcis.2022.09.091.

199 M. J. Kang, H. J. Yu, H. S. Kim and H. G. Cha, Deep eutectic solvent stabilised Co–P films for electrocatalytic oxidation of 5-hydroxymethylfurfural into 2,5-furandicarboxylic acid, *New J. Chem.*, 2020, **44**, 14239–14245, DOI: 10.1039/D0NJ01426E.

200 X. Huang, J. Song, M. Hua, Z. Xie, S. Liu, T. Wu, *et al.*, Enhancing the electrocatalytic activity of CoO for the oxidation of 5-hydroxymethylfurfural by introducing oxygen vacancies, *Green Chem.*, 2020, **22**, 843–849, DOI: 10.1039/C9GC03698A.

201 L. Gao, Z. Liu, J. Ma, L. Zhong, Z. Song, J. Xu, *et al.*, NiSe@NiO_x core-shell nanowires as a non-precious electrocatalyst for upgrading 5-hydroxymethylfurfural into 2,5-furandicarboxylic acid, *Appl. Catal., B*, 2020, **261**, 118235, DOI: 10.1016/j.apcatb.2019.118235.

202 N. Zhang, Y. Zou, L. Tao, W. Chen, L. Zhou, Z. Liu, *et al.*, Electrochemical oxidation of 5-hydroxymethylfurfural on nickel nitride/carbon nanosheets: reaction pathway determined by in situ sum frequency generation vibrational spectroscopy, *Angew. Chem.*, 2019, **131**, 16042–16050, DOI: 10.1002/ange.201908722.

203 X. Song, X. Liu, H. Wang, Y. Guo and Y. Wang, Improved performance of nickel boride by phosphorus doping as an efficient electrocatalyst for the oxidation of 5-hydroxymethylfurfural to 2,5-furandicarboxylic acid, *Ind. Eng. Chem. Res.*, 2020, **59**, 17348–17356, DOI: 10.1021/acs.iecr.0c01312.

204 M. Li, L. Chen, S. Ye, G. Fan, L. Yang, X. Zhang, *et al.*, Dispersive non-noble metal phosphide embedded in alumina arrays derived from layered double hydroxide precursor toward efficient oxygen evolution reaction and biomass upgrading, *J. Mater. Chem. A*, 2019, **7**, 13695–13704, DOI: 10.1039/C9TA03580J.

205 C. Yang, Y. Lu, W. Duan, Z. Kong, Z. Huang, T. Yang, *et al.*, Recent progress and prospective of nickel selenide-based electrocatalysts for water splitting, *Energy Fuels*, 2021, **35**, 14283–14303, DOI: 10.1021/acs.energyfuels.1c01854.

206 C. Liu, K. Wang, X. Zheng, X. Liu, Q. Liang and Z. Chen, Rational design of $MoSe_2$-NiSe@carbon heteronanostructures for efficient electrocatalytic hydrogen evolution in both acidic and alkaline media, *Carbon*, 2018, **139**, 1–9, DOI: 10.1016/j.carbon.2018.06.034.

207 Y. Huang, X. Chong, C. Liu, Y. Liang and B. Zhang, Boosting hydrogen production by anodic oxidation of primary amines over a NiSe nanorod electrode, *Angew. Chem.*, 2018, **130**, 13347–13350, DOI: 10.1002/ange.201807717.

208 M. M. Khan, S. F. Adil and A. Al-Mayouf, *Metal oxides as photocatalysts*, Elsevier, 2015, vol. 19, pp. 462–464, DOI: 10.1016/j.jscs.2015.04.003.

209 L. Gao, S. Gan, J. Ma, Z. Sun, Z. Liu, L. Zhong, *et al.*, Titanium Oxide-Confined Manganese Oxide for One-Step Electrocatalytic Preparation of 2,5-Furandicarboxylic Acid in Acidic Media, *ChemElectroChem*, 2020, **7**, 4251–4258, DOI: 10.1002/celc.202001117.

210 Y. Li, Z. Dang and P. Gao, High-efficiency electrolysis of biomass and its derivatives: advances in anodic oxidation reaction mechanism and transition metal-based electrocatalysts, *Nano Sel.*, 2021, **2**, 847–864, DOI: 10.1002/nano.202000227.

211 F. J. Holzhäuser, T. Janke, F. Öztas, C. Broicher and R. Palkovits, Electrocatalytic Oxidation of 5-Hydroxymethylfurfural into the Monomer 2,5-Furandicarboxylic Acid Using Mesostructured Nickel Oxide, *Adv. Sustainable Syst.*, 2020, **4**, 1900151, DOI: 10.1002/adsu.201900151.

212 K. E. Sickafus, J. M. Wills and N. W. Grimes, Structure of spinel, *J. Am. Ceram. Soc.*, 1999, **82**, 3279–3292, DOI: 10.1111/j.1151-2916.1999.tb02241.x.

213 H. Wang, R. Liu, Y. Li, X. Lü, Q. Wang, S. Zhao, *et al.*, Durable and efficient hollow porous oxide spinel microspheres for oxygen reduction, *Joule*, 2018, **2**, 337–348, DOI: 10.1016/j.joule.2017.11.016.

214 V. Zhandun and A. Nemtsev, Ab initio comparative study of the magnetic, electronic and optical properties of AB_2O_4 (A,

B = Mn, Fe) spinels, *Mater. Chem. Phys.*, 2021, **259**, 124065, DOI: 10.1016/j.matchemphys.2020.124065.

215 S. Lv, X. Chen, Y. Ye, S. Yin, J. Cheng and M. Xia, Rice hull/$MnFe_2O_4$ composite: preparation, characterization and its rapid microwave-assisted COD removal for organic wastewater, *J. Hazard. Mater.*, 2009, **171**, 634–639, DOI: 10.1016/j.jhazmat.2009.06.039.

216 X. Huang, J.-Y. Zhang, M. Wu, S. Zhang, H. Xiao, W. Han, *et al.*, Electronic structure and p-type conduction mechanism of spinel cobaltite oxide thin films, *Phys. Rev. B*, 2019, **100**, 115301, DOI: 10.1103/PhysRevB.100.115301.

217 A. Badreldin, A. E. Abusrafa and A. Abdel-Wahab, Oxygen-deficient cobalt-based oxides for electrocatalytic water splitting, *ChemSusChem*, 2021, **14**, 10–32, DOI: 10.1002/cssc.202002002.

218 K. Zhu, F. Shi, X. Zhu and W. Yang, The roles of oxygen vacancies in electrocatalytic oxygen evolution reaction, *Nano Energy*, 2020, **73**, 104761, DOI: 10.1016/j.nanoen.2020.104761.

219 X. Kuang, B. Kang, Z. Wang, L. Gao, C. Guo, J. Y. Lee, *et al.*, Sulfur-Doped CoO Nanoflakes with Loosely Packed Structure Realizing Enhanced Oxygen Evolution Reaction, *Chem.–Eur. J.*, 2018, **24**, 17288–17292, DOI: 10.1002/chem.201803302.

220 Y. Liu, C. Xiao, P. Huang, M. Cheng and Y. Xie, Regulating the charge and spin ordering of two-dimensional ultrathin solids for electrocatalytic water splitting, *Chem*, 2018, **4**, 1263–1283, DOI: 10.1016/j.chempr.2018.02.006.

221 J. Kim, X. Yin, K.-C. Tsao, S. Fang and H. Yang, $Ca_2Mn_2O_5$ as oxygen-deficient perovskite electrocatalyst for oxygen evolution reaction, *J. Am. Chem. Soc.*, 2014, **136**, 14646–14649, DOI: 10.1021/ja506254g.

222 D. Zu, H. Wang, S. Lin, G. Ou, H. Wei, S. Sun, *et al.*, Oxygen-deficient metal oxides: synthesis routes and applications in energy and environment, *Nano Res.*, 2019, **12**, 2150–2163, DOI: 10.1007/s12274-019-2377-9.

223 G. Li, G. R. Blake and T. T. Palstra, Vacancies in functional materials for clean energy storage and harvesting: the perfect imperfection, *Chem. Soc. Rev.*, 2017, **46**, 1693–1706, DOI: 10.1039/C6CS00571C.

224 X. Fan, Y. Liu, S. Chen, J. Shi, J. Wang, A. Fan, *et al.*, Defect-enriched iron fluoride-oxide nanoporous thin films bifunctional catalyst for water splitting, *Nat. Commun.*, 2018, **9**, 1–11, DOI: 10.1038/s41467-018-04248-y.

225 Z. Xiao, Y.-C. Huang, C.-L. Dong, C. Xie, Z. Liu, S. Du, *et al.*, Operando identification of the dynamic behavior of oxygen vacancy-rich Co_3O_4 for oxygen evolution reaction, *J. Am. Chem. Soc.*, 2020, **142**, 12087–12095, DOI: 10.1021/jacs.0c00257.

226 L. Xu, Q. Jiang, Z. Xiao, X. Li, J. Huo, S. Wang, *et al.*, Plasma-engraved Co_3O_4 nanosheets with oxygen vacancies and high surface area for the oxygen evolution reaction, *Angew. Chem.*, 2016, **128**, 5363–5367, DOI: 10.1002/ange.201600687.

227 Y. Chen, J. Hu, H. Diao, W. Luo and Y. F. Song, Facile preparation of ultrathin Co_3O_4/nanocarbon composites with greatly improved surface activity as a highly efficient oxygen evolution reaction catalyst, *Chem.–Eur. J.*, 2017, **23**, 4010–4016, DOI: 10.1002/chem.201700225.

228 H. Lei, A. Han, F. Li, M. Zhang, Y. Han, P. Du, *et al.*, Electrochemical, spectroscopic and theoretical studies of a simple bifunctional cobalt corrole catalyst for oxygen evolution and hydrogen production, *Phys. Chem. Chem. Phys.*, 2014, **16**, 1883–1893, DOI: 10.1039/C3CP54361G.

229 L. Liao, Q. Zhang, Z. Su, Z. Zhao, Y. Wang, Y. Li, *et al.*, Efficient solar water-splitting using a nanocrystalline CoO photocatalyst, *Nat. Nanotechnol.*, 2014, **9**, 69–73, DOI: 10.1038/nnano.2013.272.

230 T. E. Rosser, M. A. Gross, Y.-H. Lai and E. Reisner, Precious-metal free photoelectrochemical water splitting with immobilised molecular Ni and Fe redox catalysts, *Chem. Sci.*, 2016, **7**, 4024–4035, DOI: 10.1039/C5SC04863J.